UNIVERSITA' DI NAPOLI FEDERICO II

DOTTORATO DI RICERCA IN BIOCHIMICA
E BIOLOGIA CELLULARE E MOLECOLARE
XXIII CICLO

The relationship of the ADP-ribosylating enzyme from *S. solfataricus* with DING proteins and its intracellular localization

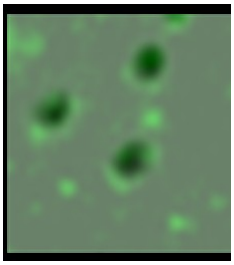

Candidate: Elena Porzio
Tutor: Prof.ssa Maria Rosaria Faraone Mennella

UNIVERSITA' DI NAPOLI FEDERICO II

DOTTORATO DI RICERCA
BIOCHIMICA E BIOLOGIA CELLULARE E MOLECOLARE
XXIII CICLO

The relationship of the ADP-ribosylating enzyme from *S. solfataricus* with DING proteins and its intracellular localization

Candidate
Elena Porzio

Tutor
Prof.ssa Maria Rosaria Faraone Mennella

Coordinator
Prof. Paolo Arcari

Academic Year 2010/2011

Alla mia famiglia
e a Salvatore

RINGRAZIAMENTI

La conclusione di questo Dottorato di ricerca è per me motivo di riflessione. Il mio rapporto con la ricerca credo sia stato segnato dall'incontro con persone, in particolare 4 donne, che hanno caratterizzato sicuramente il mio percorso formativo e lavorativo fino ad oggi, e che desidero ringraziare di cuore.

In ordine temporale, la mia Professoressa di scienze del liceo, Anna Pascucci… la sua passione, il suo entusiasmo coinvolgente per la ricerca hanno fatto nascere in me l'interesse per questo lavoro.

La mia prima esperienza in laboratorio è stata poi segnata dall'incontro con la Dr.ssa Luigia Merone, Gigia, mia guida in laboratorio durante la tesi sperimentale. Un grazie per la sua disponibilità e il suo impegno per me che non dimenticherò mai.

E poi il dottorato… ho conosciuto una donna il cui spessore personale va ancora oltre l'indiscutibile alto livello professionale: la Professoressa Maria Rosaria Faraone Mennella… la sua dedizione e passione coinvolgente per la ricerca, il suo entusiasmo, la sua correttezza e professionalità, gli insegnamenti e il forte rapporto maturato con lei, rimarranno sempre vivi in me, con grande affetto. Grazie di tutto, Prof !

E poi… la Dr.ssa Sandra Greive.. .una donna in gamba e determinata, con la quale ho condiviso un'esperienza bellissima, molto stimolante e importante per me, nel suo laboratorio in Inghilterra. Thanks a lot, Sandra!

Del laboratorio "NAD" desidero ringraziare di nuovo la Prof.ssa Faraone Mennella, in particolare per la sua fiducia in me e la serenità che mi ha trasmesso nel lavoro di questi anni.

Ringrazio con affetto la Dr.ssa Anna De Maio. Grazie Anna per la disponibilità, l'aiuto e l'allegra atmosfera che hai sempre creato.

Grazie alla Prof.ssa Benedetta Farina, la cui affettuosa presenza è stata sempre di supporto negli anni.

Un affettuoso Grazie va a Melania, mia collega di questa avventura, con la quale ho condiviso con piacere tutte le esperienze di questi anni, più o

meno faticose, più o meno divertenti, sempre in piena armonia e basate su una sincera amicizia, che rimarrà per sempre.
Desidero ringraziare e ricordare tutti i ragazzi che hanno svolto la loro tesi sperimentale con me; grazie a loro ho imparato molto anch'io, e di ognuno porterò un caro ricordo… Valentina, Massimiliano, Valentina A., Eleonora, Andrea, Margherita, Teresa, Maria e Rossella…. insieme a Consuelo, Elena, Lucia e tutti coloro con cui ho condiviso qualche esperienza.

Infine voglio ringraziare le persone più importanti della mia vita, a cui dedico questo lavoro. La mia famiglia, in particolare mia madre: grazie per l'amore e l'aiuto incondizionato che mi ha permesso di dedicare molto più tempo al lavoro; grazie a mio padre, i cui silenziosi insegnamenti, basati sull'esempio di correttezza e dedizione nel lavoro, hanno da sempre ispirato i miei comportamenti; grazie a mia sorella Carla, la cui presenza indispensabile mi ha affiancato in questi anni; e grazie a te, Salvatore, che hai sempre rispettato, (e a volte sopportato!!!) ma comunque consigliato e appoggiato le mie scelte, dandomi un'indispensabile carica e serenità.

SUMMARY

The PARP*Sso* thermoprotein from *Sulfolobus solfataricus* has been identified as a PARP-like enzyme that cleaves β-NAD^+ to synthesize oligomers of ADP-ribose and cross-reacts with polyclonal anti-PARP-1 catalytic site antibodies. Despite the biochemical properties that allow to correlate it to PARP enzymes, the N-terminal and partial amino acid sequence suggest the sulfolobal enzyme belongs to a different class of enzymes, the DING proteins. Considering the high sequence identity with the human DING protein HPBP and the lack of a nucleotide coding sequence in both human and sulfolobal genomes, we hypothesized that PARP*Sso* might share other features with the human DING. Further analysis of PARP*Sso* amino acid sequence addressed the research towards studying other possible similarities between human and sulfolobal protein and then to explain how PARP*Sso* correlates with canonic PARPs. For the latter question, the peculiar behaviour of the thermozyme, that is biochemically, but not structurally related to the classic PARPs, stimulated to investigate by computational analysis and databank, whether the protein might be phylogenetically related to any already known PARP amino acid sequence.

Moreover, immunochemical and enzymatic crossed analyses were performed to establish whether purified HPBP and PARP*Sso* have common immunoreactive and functional behaviour.

The second part of the research was focused on the localization of PARP*Sso* within the sulfolobal cell. Our interest to this item arose from the property of some DING proteins to be membrane bound, suggested to work as membrane transporters. On the other hand, from previous studies, it is known that PARP*Sso* is only partially solubilized from the starting cell homogenate provided by ICMIB (CNR), and the soluble enzyme is strictly associated with DNA. In this thesis work, whole cells collected by centrifugation from culture medium were subjected to a different extraction procedure. This procedure included also experimental conditions used to differentiate between soluble (i.e. cytoplasmic) and insoluble (i.e. membrane-bound) protein fractions. PARP*Sso* and DNA distributions were determined by enzyme assay, immunoblotting and agarose gel electrophoresis. Reciprocal interactions of thermozyme, nucleic acid and membrane lipids were investigated with different techniques and methodologies (nucleoid preparation, fluorescence binding assays, fluorescence microscopy analysis).

RIASSUNTO

La termoproteina PARP*Sso* da *Sulfolobus solfataricus* è stata identificata come un enzima di tipo poli-ADP-ribosilante che utilizza β-NAD^+ come substrato per sintetizzare oligomeri di ADP-ribosio, e reagisce con anticorpi policlonali anti-sito catalitico della PARP-1.
Nonostante le proprietà biochimiche permettano di correlarla ad enzimi PARP, la parziale sequenza amminoacidica e la sequenza N-terminale indicano che l'enzima sulfolobale appartiene ad una diversa classe di enzimi, le proteine DING. Considerando l'elevata identità di sequenza con la proteina DING umana, HPBP, e la mancanza di una sequenza nucleotidica codificante in entrambi i genomi umano e sulfolobale, si ci è chiesti se PARP*Sso* potesse condividere altre caratteristiche con la DING umana. Ulteriori analisi della sequenza amminoacidica della PARP*Sso* hanno indirizzato la ricerca verso lo studio di altre possibili similitudini tra la proteina umana e sulfolobale, e successivamente a spiegare come la PARP*Sso* si correli alle canoniche PARPs. In merito a quest'ultimo quesito, il peculiare comportamento del termozima, che è correlato dal punto di vista biochimico, ma non strutturale alle classiche PARP, ha spinto ad indagare, mediante analisi computazionale e in banca dati, se la proteina potesse essere filogeneticamente correlata alla sequenza di qualche già nota PARP. Inoltre sono state effettuate analisi immunochimiche ed enzimatiche incrociate per valutare se le proteine purificate HPBP e PAR*Sso* avessero un comportamento comune dal punto di vista immunochimico e funzionale.
La seconda parte della ricerca si è concentrata sulla localizzazione della PARP*Sso* nelle cellule sulfolobali. L'interesse verso questo aspetto è sorto considerando che alcune proteine DING sono legate a membrana, suggerendone un ruolo come trasportatori di membrana. D'altra parte, da studi precedenti, è noto che l'enzima PARP*Sso* è solo parzialmente solubilizzato a partire dall'omogenato cellulare fornito dall'ICMIB (CNR), e che l'enzima solubile è strettamente associato al DNA.
Nel presente lavoro di tesi, cellule intere di *S. solfataricus*, raccolte per centrifugazione a partire da una coltura cellulare, sono state sottoposte a una diversa procedura di estrazione. Tale procedura ha previsto anche condizioni sperimentali utilizzate per distinguere frazioni contenenti proteine solubili (es. citoplasmatiche) e insolubili (es. di membrana).
La distribuzione della PARP*Sso* e del DNA è stata determinata con saggi enzimatici ed analisi mediante immunoblotting e elettroforesi su gel d'agarosio. Le interazioni reciproche di termozima, acido nucleico e lipidi di membrana sono state studiate con diverse tecniche e metodologie

(preparazione del nucleoide, saggi di legame in fluorescenza, analisi di microscopia a fluorescenza).

INDEX

LIST OF TABLES AND FIGURES

INTRODUCTION

1.1 The poly-ADP-ribosylation reaction and the PARP family

In eukaryotic cells poly-ADP-ribosylation is a widespread post-translational modification of proteins catalysed by a family of NAD^+ ADP-ribosyl transferases, the poly-ADP-ribose polymerases (PARPs) (Hassa *et al.*, 2008). PARPs utilize NAD^+ molecule as substrate to transfer successive ADP-ribose units to glutamic or aspartic acid residues of target proteins, giving rise to long and branched ADP-ribose polymers (Amé *et al.*, 2004).

The poly-ADP-ribosylation reaction can be divided in various phases:

- break of the N-glycosidic bond between nicotinamide and ribose, with release of the nicotinamide and attachment of the first adenosine diphosphate ribose unit (ADPR) to glutamic or aspartic acid residues via an ester linkage.
- Elongation of the linear chain by 1''→2' ribose-ribose glycosidic bonds between ADPR units, (synthesis of a linear polymer, up to 200 units).
- Branching of the polymer every 20–50 units (Hayashi K. *et al.*, 1983), (Figure 1).

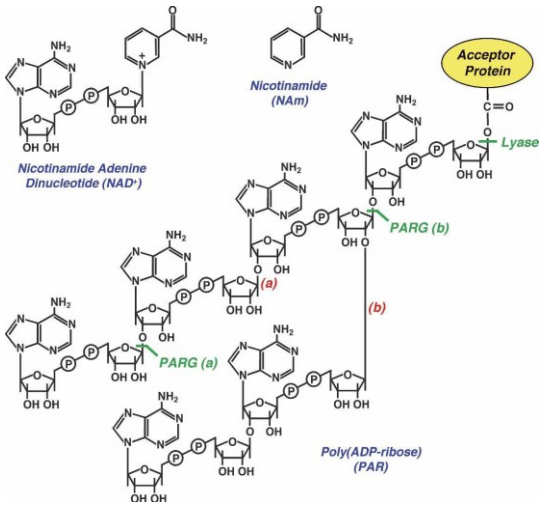

Figure 1: Chemical structures of NAD^+, nicotinamide (NAm) and poly ADP-ribose (PAR). The degradation of PAR is catalyzed by PARG, which has both exoglycosidase (*PARG(a)*) and endoglycosidase activity (*PARG(b)*). Remaining protein-proximal ADP-ribose is removed by ADP-ribosyl protein lyase.

The PARP family comprises 18 known members identified by homology searching and *in silico* characterization (Amé *et al.*, 2004; Otto *et al.*, 2005), that share homology with the catalytic domain of the founding member, PARP-1.
PARP-1 has a highly conserved structural and functional organization including (Figure 2):

- a N-terminal DNA-binding domain (DBD) with two zinc finger motifs (FI and FII) that act as "nick sensor" and recognise DNA damage (D'Amours *et al.*, 1999) and a third one recently identified (Langelier *et al.*, 2008), that mediates interdomain contacts important for DNA-dependent enzyme activation. Two helix-turn-helix motifs are also contained within the PARP-1 DBD and are essential for its binding to DNA;
- a nuclear localization signal (NLS) that targets PARP-1 to the nucleus (Schreiber *et al.*, 1992);
- a central auto-modification domain containing a BRCT motif as well as several glutamic acid residues for PAR binding (Desmarais *et al.*, 1991). The BCRT domain mediates PARP-1 homodimerisation and its interaction with other protein partners (heterodimerisation);
- a C-terminal catalytic domain with a contiguous 50-amino-acid sequence, the "PARP signature" motif, that forms the active site.

All the members belonging to the PARP family have different size, cellular localization and role: the most known PARP-1 and PARP-2, PARP-3, tankirase1, vPARP are localized in different subcellular sites, respectively nucleus, centrosomes, telomers and vaults particles in cytoplasm (Paul *et al.*, 2005). Some of the recently discovered PARPs (PARP-6, PARP-16 and PARP-10) seem to be closer to ADP-ribosyl transferases, as they catalyze mono-ADP-ribosylation, (Kleine *et al.*, 2008). Hottiger e*t al.* proposed a new nomenclature based on sequence and structure homology search of the conservative ADP-ribosyltransferase fold (Figure 3), and enlarged the family of ADP-ribosylating enzymes by including in it mono- and poly- ADP-ribosylation proteins, and named all members as ARTs (Hottiger *et al.*, 2010).

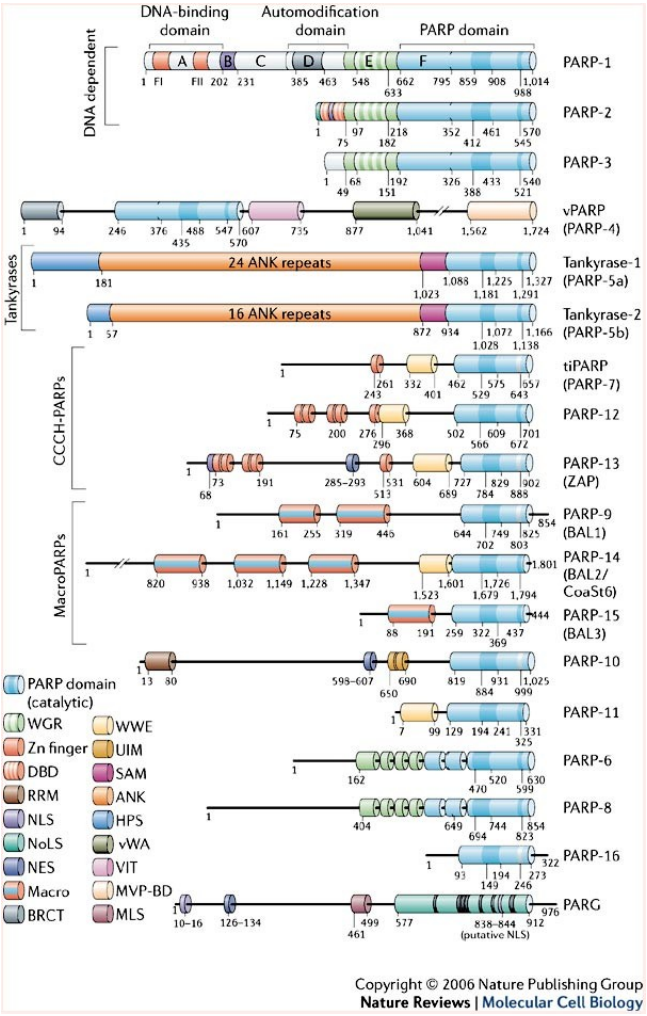

Figure 2: Classical schematic representation of domain structures of the PARP family members.
The meaning fo single domains is explained in Figure 3.

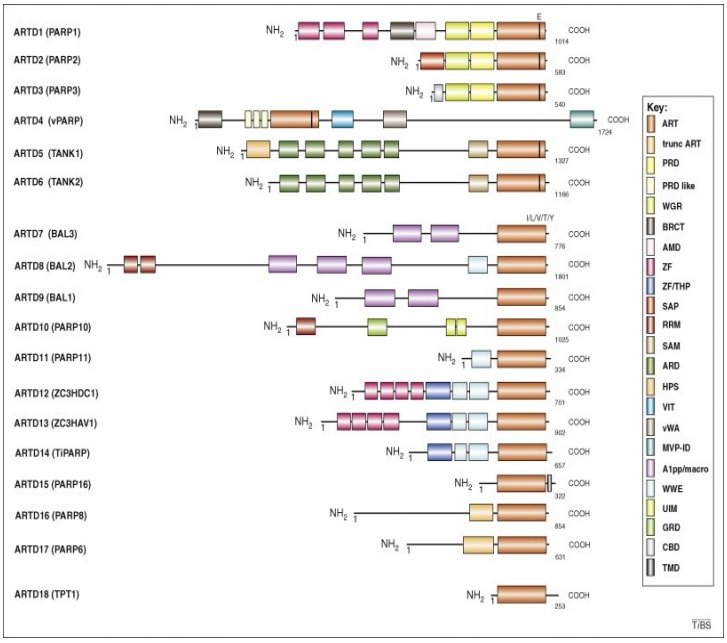

Figure 3: A new schematic comparison of the functional domains of the human ARTD (PARP) family.
The most relevant are: **ART**, is the catalytic core required for basal ART activity. PARP regulatory domain (**PRD**) might be involved in regulation of the PARP-branching activity. **WGR**, characterized by the conserved central motif (W-G-R), is also found in a variety of polyA polymerases and in proteins of unknown function. **BRCT** domain (BRCA1 carboxy-terminal domain) is found within many DNA damage repair and cell cycle checkpoint proteins. **Macro** domain can serve as ADPr or O-acetyl-ADPribose binding module. **ZF**: zinc finger domains, recognizing DNA breaks (Hottiger *et al.*, 2010).

Only two out of the eighteen PARP family members are activated in response to DNA damage, PARP-1 and PARP-2 (Amé *et al.*, 1999).
The 113 kDa PARP-1 is the most abundant PARP enzyme found in living cells, with an average 1.0×10^6 molecules per cell (Yamanaka *et al.*, 1988; D'Amours *et al.*, 1999), and accounts for at least 85% of the cell PARP activity (Shieh *et al.*, 1998). both of them are activated for PAR polymer synthesis on binding to DNA strand breaks, and are involved in single-strand break (SSB), double strand break (DS) and base excision (BE) repair. Cell PAR levels are increased up to 500-fold following DNA damage induction (Benjamin, R.C., Gill, D.M., 1980; Menissier-de Murcia *et al.*, 1989). PARP binds to DNA containing single-strand breaks

as a homodimer resulting in its activation. One monomer is then able to auto-modify the other, leading to an accumulation of negative charge and causing repulsion of the dimer from the DNA (Ferro, A.M., Olivera, B.M., 1982; Woodhouse B. C., Dianov G. L., 2008) (Figure 4). This auto-modification also inhibits both ADP-ribosyl transferase and protein–protein interaction activities of PARP (D'Amours *et al.*, 1999).

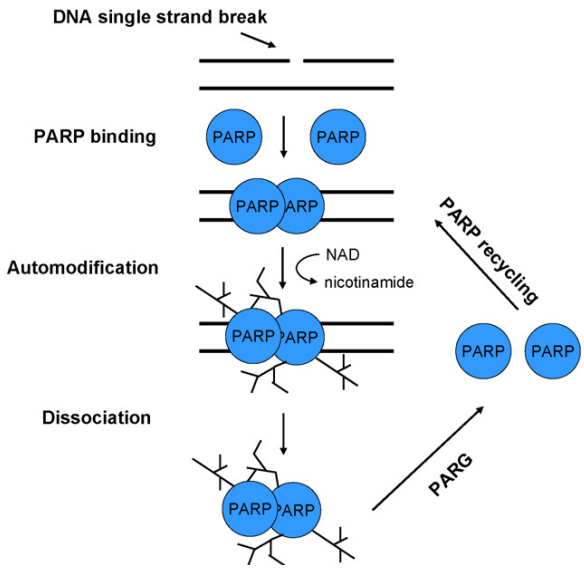

Figure 4: Mechanism of action of PARP-1 in the presence of DNA strand breaks.

Moreover the molecular mechanism of BER may involve a local chromatin relaxation mediated either by covalent modification of histones with poly-ADP-ribose or by non-covalent interaction of histones with poly-ADP-ribose that automodifies the enzyme. This regulates the accessibility to other DNA repair proteins. In addition PARP-1 has been shown to directly recruit repair protein like XRCC1 (X-ray repair cross-complementing 1) to the site of DNA damage (El-Khamisy *et al.*, 2003).

The metabolism of PAR is a dynamic process involving also its degradation. In humans two genes have been identified whose products exhibit poly-ADP-ribose glycohydrolase (PARG) activity, namely PARG and more recently ARH3. The PARG gene encodes the predominant long nuclear/cytoplasmic isoform (~110 kDa) and, by alternative splicing, a

short catalytically active cytoplasmic isoform (~65 kDa), (Meyer-Ficca *et al.*, 2004). Recently in mammals it has been reported the existence of a second 39 kDa protein, ARH3, exhibiting PARG-like activity (Oka *et al.*, 2006). Even if they are structurally unrelated, these enzymes hydrolyze the glycosidic bonds of PAR polymers to generate free ADP-ribose, leaving the protein-proximal ADP-ribose monomers to be removed by ADP-ribosyl protein lyase (Figure 1).

1.2 *Sulfolobus solfataricus* and the PARP*Sso* enzyme

Sulfolobus solfataricus belongs to Archaea which, together with Eukarya and Eubacteria kingdoms, represents the third domain of living organisms (Woese *et al*., 1990).
Although present in several vulcanic areas, *S. solfataricus* was first isolated from an acidic hot spring in Agnano (Napoli, Italy). It is a thermophilic sulphur-dependent archaeon living optimally at 87 °C and pH 3.5 (De Rosa *et al.*, 1975), even if it has a neutral cytoplasmic pH around 6.5-7.0.
The particular biochemical composition of the membrane, including lipids with tetraethers bonds forming a monolayer (Gambacorta *et al.*, 2004), confers them great impermeability and resistence to high temperature and extreme conditions (Limauro *et al.*, 2004).
The genome of the crenarchaeon *Sulfolobus solfataricus* P2 contains about $3x10^6$ bp on a single chromosome and putatively encodes 2977 proteins. One-third of the encoded proteins have no detectable homologs in other sequenced genomes. Moreover, 40% appear to be archaeal-specific, and only 12% and 2.3% are shared exclusively with bacteria and eukarya, respectively (She *et al.*, 2001). Although the latter percentage seems to be very low, and Archaea are morphologically similar to eubacteria, it's important to underline that the members of the genus *Sulfolobus,* possess trancription and translation factors similar to those found in eukaryotes (Sutrave *et al.*, 1994; Keeling, P.J., Doolittle, W.F., 1995).

In the laboratory where the research project of this thesis has been carried out, a poly-ADP-ribose polymerase (PARP)-like thermoprotein, PARP*Sso*, was found in *Sulfolobus solfataricus* (Faraone-Mennella *et al.*, 1998), representing the first evidence of an ADP-ribosylation activity in Archaea.
Scheme 1 shows the main properties of PARP*Sso* and differences from human PARP-1 (116kDa): lower molecular mass (46.5kDa) and isoelectric point (pH 7.0-7.2), and high thermophily (80°C). The thermozyme cleaves β-NAD^+ to synthesize short ADP-ribose oligomers (5-6 units) and cross-reacts with both polyclonal anti-PARP-1 catalytic site and anti-poly-ADP-ribose polymerase antibodies, but not with anti-DNA-binding PARP-1-N-terminus antibodies (Faraone-Mennella *et al.*, 1998). Similarly to eukaryotic PARP-1, PARP*Sso* is activated by and binds DNA with high affinity and non-specifically (Faraone-Mennella *et al.*, 2002), modifies itself (automodification) and a 7kDa protein (Sso7)

(heteromodification) that binds and condenses archaeal DNA (Faraone-Mennella *et al.*, 1995; Castellano *et al.*, 2009).

Scheme 1: Biochemical features of PARP*Sso* and PARP-1

	PARP*Sso*	PARP-1
Size	46.5 kDa	116 kDa
Optimum temperature	80°C	25°C
Isoelectric point	7.1	9.5
K_M NAD	150±50 μM	20-80 μM
Activators	Mg^{2+}	Mg^{2+}
3-ABA inhibition	50%	100%
ADPR chain length	4-5 residues	Up to 200 residues
Anti-PARP immunoreactivity	+	+
DNA binding ability	+	+
Automodification	+	+
Heteromodification	+	+

Although PARP*Sso* has been characterized biochemically, in the whole genome of *S. solfataricus* (strain P2) no gene sequence has been found, corresponding to classic PARPs.
Recently the partial amino acid sequence of PARP*Sso* clearly indicated that the analysed PARP*Sso* N-terminus and tryptic peptides (about 60% of total residues) do not share structural similarity with any of known PARPs, but the peculiar feature of N-terminus (40 residues) overlaps those of DING proteins, as shown in the alignment of Figure 5 (Di Maro *et al.*, 2009). This is the first example of a DING protein from *Sulfolobus solfataricus* and, in general from Archaea.

```
PARPSso       --DINGGGATLPQKLYQTSGVLTAGFAPYIGVGSGNGKAAFLTNDYTK------------ 45
ZP_00138283   MADINGGGATLPQQLYQEPGVLTAGFAAYIGVGSGNGKAAFLNNDYTKFVAGTTNKNVHW 60
2CAP_A        --DIDGGGATLPEKLYLTPDVLTAGFAPYIGVGSGKGKIAFLENKYNQFGTDTT-KNVHW 57
P27SJ         MADINGGGATLPQALYQTSGVLTAGFAPYIGVGSGNGKAAFLNNDYTKFQAGVTNKNVHW 60
                **:*******: **  ..*******.*******:** *** *.*.:
                     ©©                      ©

PARPSso       ------LTAT-ELSTYATNLQPTWGKLIQVPSVATSVAIPFR------------------ 80
ZP_00138283   AGSDSKLSKTNETNPYLSAHGSAWGPLIQVPSVATSVALPFNKSGSNAVNFADVNTLCGV 120
2CAP_A        AGSDSKLTAT-QLATYAADKEPGWGKLIQVPSVATSVAIPFRKAGANAVDLS-VKELCGV 115
P27SJ         AGSDSKLSAT-ELSTYASAKQPTWGKLIQVPSVGTAVAIPFNKSGTAAVDLS-VSELCGV 118
                  **: * :  .* :   . ** *******.*:**:**:
                ©

PARPSso       ----ITDWSGISGAGRTGPITVVYR---------------------------------- 102
ZP_00138283   FSGRLTDWSQIPGSGRSGAITVVYRSESSGTTELFTRFLNASCSSTLEGGTFAITTSFGS 180
2CAP_A        FSGRIADWSGITGAGRSGPIQVVYRAESSGTTELFTRFLNAKCTT--QPGTFAVTTVFAN 173
P27SJ         FSGRITDWSGISGSGRTGAITVVYRSESSGTTELFTRFLNAKCA---ETGTFNISTTFGT 175
                  ::*** *.*:**:*.* ****
                                    ©   ©©©

PARPSso       --------------------------------ITYMSPDFAASTLAGLDDATKGVSPA 128
ZP_00138283   SFSGGLP--AGAVSAQGSQAVMNALNA---AQGRITYMSPDFAAPTLAGLDDATKVAQVR 235
2CAP_A        SYSLGLTPLAGAVAAIGSDGVMAALNDTTVAEGRITYISPDFAAPTLAGLDDATKVARTG 233
P27SJ         SYTGGLP--AGAVSAAGSQGVMTALAG---ADGGTTYMSPDFAAPTLAGLDDATKVARVG 230
                                                **:******.********** .

PARPSso       P---------------SNVSDAIAQVLPPNDPS-------APLDVTNPDDGVAGVQPYPD 166
ZP_00138283   G----------VSPAPANVSAAIGAVTPPTTAQRSDPNNWVPVFAATANPNDPSVRPYPT 285
2CAP_A        KGVVSGVAVEGKSPAAANVSAAISVVPLPAAADRGNPDVWVPVFGATTGG---GVVAYPD 290
P27SJ         ----------------KDVATNTAGVSP-AAANVSAAINAVPVPASTEKP---------- 263
                              :*:   . *     ..       .*:  :.      .* .**

PARPSso       SGYPILGFTNLIFS-------------AFFTKHFGDTNNNDDAITANRFVPLPDNWK    210
ZP_0013823    SGYPILGFTNLIFSQCYANATQTQQVRDFFTRHYGATANNDTAITNHRFVPLPASWKLAV 345
2CAP_A        SGYPILGFTDLIFSECYANATQTGQVRDFFTKHYGTSANDNAAIEANAFVPLPSNWKAAV 350
P27SJ         ------------------------------------------------------------
              *********:****              ***:*:* : *:: **  : ***** .**

PARPSso       -------------------------
ZP_00138283   RQSFLTSTNNLYIGHSNVCNGIGRPL 371
2CAP_A        RASFLTASNALSIGNTNVCNGKGRPE 376
P27SJ         -------------------------
```

Figure 5: Partial amino acid sequence of PARP*Sso* (in bold font).
A multiple alignment between **PARP*Sso***, DING proteins from *Pseudomonas fluorescence* (**ZP_00138283)**, human (**2CAP_A**), and plant *Hypericum perforatum* (**p27SJ**) is shown. Identical residues (*), conserved substitutions (:) and semi-conserved substitutions (.) are reported. The conserved residues involved in phosphate-binding site in DING proteins are also indicated (©).

1.3 DING proteins

The DING proteins (38–40 kDa) are ubiquitous proteins, characterized by a conserved N-terminal sequence, DINGGG (Berna *et al.*, 2009). In 1990s they were first identified in several animal and plant tissues, and then in most eukaryotes and a range of bacterial organisms (Berna *et al.*, 2002). At present the DING family includes about 30 members.

DING proteins are usually secreted, although some are sometimes found in the cytosol (Luecke *et al*., 1990; Berna *et al.*, 2002). Their roles are not completely clearied yet; however the ability to bind phosphate seems to be a common property, confirmed by three-dimensional structure analysis of both eukaryotic and prokaryotic DING proteins (Berna *et al.*, 2009). Except for one prokaryotic DING protein, no complete gene sequences have been identified in all the eukaryotic genome databases.

1.3.1 DING proteins in Prokaryotes

In prokaryotes DING proteins are part of a superfamily of phosphate-binding proteins that comprises three sub-groups, based on sequence similarities and functions:

1. ubiquitous membrane-bound or periplasmic **Psts proteins** that participate in phosphate uptake and belong to transmembrane ABC transporters. These periplasmic proteins haven't the characteristic N-term sequence, but show 20-25% identity with the eukaryotic DING proteins;
2. some low relative molecular weight (M_r) **alkaline phosphatases** only described in *Pseudomonas*;
3. **true bacterial DING proteins** that share around 70-80% identity with the eukaryotic ones (Berna *et al.*, 2008).

The gene for one such protein, *Pflu*DING *from P. fluorescens* SBW25, has been cloned and expressed in *Escherichia coli* (Scott K, Wu L., 2005). It binds a single phosphate ion, but has no detectable phosphatase activity. It is an extracellular protein, which expression is linked to low extracellular phosphate levels. This suggests that *Pflu*DING could be involved in extracellular scavenging of phosphates, which are subsequently taken up by the cell-bound Pst transport system (Zhang *et al.*, 2007). PstS and DING proteins co-exist in some *Pseudomonas* strains, which they confer a highly adhesive and virulent phenotype to.

Recently in the thermophilic bacterium *Thermus thermophilus* it has been identified a phosphatase with a tipical DING N-terminal sequence that interacts with the cell membrane. It has a molecular weight of 40 kDa, and exhibits optimal phosphatase activity at pH 12.3 and 70 °C. This DING protein is a multifunctional enzyme with ATPase, endonuclease and 3'-phosphodiesterase activities; moreover it binds to linear dsDNA, displaying helicase activities and could thus be involved in DNA repair (Pantazaki *et al.*, 2008).

1.3.2 DING proteins in Eukaryotes

In eukaryotes DING proteins have been identified in animals (human, monkey, rat, turkey), plants (*Hypericum perforatum*, *Arabidopsis thaliana*, potato, tobacco) and fungi (*Candida albicans*, *Ganoderma lucidum*) (Berna *et al.*, 2008; Darbinian-Sarkissian *et al.*, 2006) mostly as a 40 kDa protein or higher molecular weight DING proteins (Perera *et al.*, 2008). In particular in mice, DING proteins are present as isoforms of various molecular weights. Their intracellular localization is tissue-dependent, being exclusively nuclear in neurons, but both cytoplasmic and nuclear in other tissues (Collombet *et al.*, 2010).
Some of these proteins seem to have key roles in various human diseases, e.g., rheumatoid arthritis, atherosclerosis, HIV suppression. Although this protein family seems to be ubiquitous in eukaryotes, their genes are consistently lacking from genomic databases (Berna *et al.*, 2009).
The only eukaryotic DING protein with a complete amino acid sequence is HPBP, the Human Phosphate Binding Protein. It is a serendipitously discovered plasma apolipoprotein that binds phosphate and is isolated from human plasma (Contreras-Martel *et al.*, 2006). It forms hetero-oligomers that stabilize paraoxonase (PON1), a plasma enzyme known for its anti-atherogenic properties (Shih *et al.*, 1998); HPBP could thus be indirectly involved in protection against atherosclerosis (Rochu *et al.*, 2007; Rochu *et al.*, 2008).
HPBP structure was solved (Morales *et al.*, 2006) and it has confirmed the structural homology with bacterial PstS one; it corresponds to a "Venus flytrap" model, in which two globular domains hinge together to create a phosphate-binding site between them, comprising the eight well conserved amino acid residues (Berna *et al.*, 2008).
Three other human DING proteins involve the crystal adhesion inhibitor (CAI), the human synovial stimulatory protein (SSP), and the X-DING-$CD4^+$ from human $CD4^+$ T lymphocytes (Lesner *et al.*, 2009).

Although the amount of data concerning this protein family has increased over the last few years, their physiological functions remain largely unknown, and their origin in eukaryotes is still under debate (Berna *et al*., 2009).

1.3.3 DING proteins in Archaea

The recent partial amino acid sequence of PARP*Sso* clearly indicated that the sulfolobal thermozyme is a DING protein. The thermostable poly-ADP-ribose polymerase-like enzyme from *Sulfolobus solfataricus* has the characteristic DING N-terminal sequence and represents the first example of the archaeal DING protein; this finding extends the existence of DING proteins to the third kingdom of life (Di Maro *et al.*, 2009).

1.4 Scientific hypothesis and aim of the work

The PARP*Sso* thermoprotein from *Sulfolobus solfataricus* has been identified as a PARP-like enzyme that cleaves β-NAD^+ to synthesize oligomers of ADP-ribose and cross-reacts with polyclonal anti-PARP-1 catalytic site antibodies.
Despite the biochemical properties that allow to correlate it to PARP enzymes, the N-terminal and partial amino acid sequence suggest the sulfolobal enzyme belongs to a different class of enzymes, the DING proteins.
Considering the high sequence identity with the human DING protein HPBP and the lack of a nucleotide coding sequence in both human and sulfolobal genomes, we hypothesized that PARP*Sso* might share other features with the human DING. Further analysis of PARP*Sso* amino acid sequence, addressed the research towards studying other possible similarities between human and sulfolobal protein, then to explain how PARPSso correlates with canonic PARPs. For the latter question, the peculiar behaviour of the thermozyme, that is biochemically, but not structurally related to the classic PARPs, stimulated to investigate by computational analysis and databank, whether the protein might be phylogenetically related to any already known PARP aa sequence.
Moreover, immunochemical and enzymatic crossed analyses were performed to establish whether purified HPBP and PARP*Sso* have common immunoreactive and functional behaviour.
The second part of the research was focused on the localization of PARPSso within the sulfolobal cell. Our interest to this item arose from the property of some DING proteins to be membrane bound, suggested to work as membrane transporters. On the other hand, from previous studies, it is known that PARP*Sso* is only partially solubilized from the starting cell homogenate provided by ICMIB (CNR), and the soluble enzyme is strictly associated with DNA. In this thesis work, whole cells collected by centrifugation from culture medium were subjected to a different extraction procedure. This procedure included also experimental conditions used to differentiate between soluble (i.e. cytoplasmic) and insoluble (i.e. membrane-bound) protein fractions. PARP*Sso* and DNA distribution were determined by enzyme assay, immunoblotting and agarose gel electrophoresis. Reciprocal interactions of thermozyme, nucleic acid and membrane lipids were investigated with different techniques and methodologies (nucleoid preparation, fluorescence binding assays, fluorescence microscopy analysis).

MATERIALS AND METHODS

2.1 Materials

Nicotinamide adenine dinucleotide di(triethylammonium)salt (adenylate-^{32}P), [^{32}P]NAD^{+}, 1000 Ci/mmol, was supplied by GE Healthcare Europe GmbH, Bio-Sciences; DNase I (EC 3.1.21.1), phenylmethyl sulphonyl fluoride (PMSF), phosphatase substrate were obtained from SIGMA Chemical Company (Milan, Italy). Electrophoretic markers were purchased from BioRad (Milan, Italy).

2.2 Human and sulfolobal protein crude extracts and DING proteins purification

S. solfataricus (strain MT-4, DSM No. 5833) cells were grown at 87°C (pH 3.5) and the crude homogenate was prepared from the collected cells as described in Faraone Mennella *et al*., 1998. All protein solutions contained a cocktail of protease inhibitors (2 μg/ml). PARP*Sso* was purified by a two-step chromatographic protocol starting from a crude extract obtained digesting the crude homogenate with DNase I (Faraone Mennella *et al*., 1998). Protein concentration was determined by Bradford protein assay.
For PARP*Sso* analysis from sulfolobal cells, grown on yeast (Y) and glucose (G) medium, at exponential (E) and stationary (S) phase, 1 O.D.$_{600}$ of each culture was centrifuged at 6000 rpm for 20 min and the pellet suspended with assay buffer (100 μl; § 2.7); aliquots (10 μl) were used for enzymatic assay and SDS-PAGE analysis.
Human sera were provided by the transfusional centre of the Hospital "Agostino Maresca" in Torre del Greco (Naples, Italy).
Purifed DING protein HPBP was provided by Chabriere's group (Marseille Universite´, Marseille, France; Contreras-Martel *et al.*, 2006).

2.3 SDS-PAGE and immunoblotting

Proteins were analyzed on 12% polyacrylamide slab gels in the buffer system Tris-Glycine in the presence of 0.1% SDS as described previously (Faraone Mennella *et al*., 1998) and electrotransferred onto PolyVinyliDene Fluoride (PVDF) membrane (Bio Rad) at 200 mA for 2 hours at 4°C in the same buffer used for the electrophoretic run with 0.025% SDS.

Staining was in 0.1% Coomassie R-250, in 10% acetic acid and 45% methanol. Gels were destained in 10% acetic acid and 10% ethanol solution.
Silver staining was performed according to procedure described in Rabilloud, T., 1992.
Images of stained gels, filters and autoradiographic patterns were acquired by a phosphor imager (mod. FX, Bio-Rad).
For immunoblot experiments, procedures and buffers were as previously described (Faraone Mennella *et al*., 1998). PVDF sheets were treated for 1.5 hr with the blocking solution, TBST (50 mM Tris-HCl, pH 8.0, 150 mM NaCl, 0.5 % (v/v) Tween 20), and 3 % (w/v) gelatine. Incubation with primary antibody (used antibodies are listed in Table 1) was performed for 2 hr at room temperature in the same solution supplemented with 0.3 % gelatine.
The blots were then washed several times with TBST buffer and antibody binding was detected by using horseradish peroxidase (HRP)-conjugated secondary antibody, specific for each primary antibody, after incubation for 1 hr at room temperature. HRP reaction was revealed by using a kit for chemiluminescence (Super Signal West Dura Extended Substrate, 34075, PIERCE) and measured by the phosphor imager (BioRad).

TABLE 1: Main characteristics of specific anti-PARP and anti-DING proteins antibodies.
Dilution and secondary antibodies (AbII) used are also indicated.

Ab I	epitope	diluition	Ab II
Anti-PARP-CS	C-terminal domain of PARP-1	1:1000	Anti-rabbit 1:2000
Anti-PAR (poliADPR)	5-200 units ADPR	1:1000	Anti-rabbit 1:2000
Anti-DING N-term	N-terminal sequence (1-18 aa) of HPBP	1:1000	Anti-rabbit 1:2000
Anti-4D7 monoclonal	4D7 sequence of HPBP	1:2000	Anti-mouse 1:2000
Anti-BH6 monoclonal	8H6 sequence of HPBP	1:2000	Anti-mouse 1:2000
Anti-poliC	whole sequence of HPBP	1:2000	Anti-rabbit 1:2000
Anti-*Pflu*DING	whole sequence of DING from *P. fluorescens*	1:5000	Anti-rabbit 1:2000

A stripping procedure was used to remove antibodies from the western blot membranes, to allow incubation with other antibodies. Stripping buffer contained 62.5 mM Tris-HCl (pH 6.8), 2% SDS and a final concentration of 0.1 M 2-mercaptoethanol. The filter was washed in TBST (3 x 5 min) and incubated in stripping buffer for 1h and 50 min at 60°C (in a heating oven). Washes in TBS (5 x 10 min) followed and the membrane was blocked for 1.5 h in TBST/3% gelatine. The filter was used for developing the next immunoblot.

2.4 Alkaline filter treatment

To detache PAR from the protein immobilized on PVDF membrane, after the stripping procedure, the filter was incubated overnight in 20 mM Tris/HCl pH 8.0 at 4°C. Then it was washed in

TBST buffer (3 x 5 min) and incubated again for immunoblot with anti-PAR antibodies.

2.5 Protein sequencing by mass spectrometry

2.5.1 *Electrophoresis fractionation and in situ digestion*

The protein mixture was fractionated by gel electrophoresis. Selected protein bands stained by Colloidal Comassie were excised from the gel and washed in 50 mM ammonium bicarbonate pH 8.0 in 50% acetonitrile to a complete destaining. The gel pieces were re-suspended in 50mM ammonium bicarbonate pH 8.0 containing 100 ng of trypsin and incubated for 2 hr at 4°C and overnight at 37°C. The supernatant containing the resulting peptide mixtures was removed and the gel pieces were re-extracted with acetonitrile. The two fractions were then collected and freeze-dried.

2.5.2 *MALDI MS and MALDI MSMS analysis*

MALDI mass spectra were recorded on an Applied Biosystem 4800 plus MALDI TOF-TOF Analyzer mass spectrometer equipped with a reflectron analyser and used in delayed extraction mode with 4000 Series Explorer v3.5 software. Aliquot of 0.5µl of peptide sample was mixed with an equal volume of α-cyano-4-hydroxycynnamic acid as matrix (10 mg/ml in 0.2% TFA in 70% acetonitrile), applied to the metallic sample plate and air dried. Mass calibration was performed by using the standard mixture provided by manufacturer

MALDI-MS data was acquired manually over a mass range of 600–5000 Da in the positive-ion reflector mode. In each MS spectrum, specific MS peaks were selected for manual MS/MS analysis, using a 1 kV MS/MS operating mode.

2.5.3 *LCMSMS analysis*

The aliquot of peptide mixtures were further analyzed by LCMSMS using a LCMSMS using the LC/MSD Trap XCT Ultra (Agilent Technologies, Palo Alto, CA) equipped with a 1100 HPLC system and a chip cube (Agilent Technologies). After loading, the peptide mixture (8 µl in 0.5% TFA) was first concentrated at 4 µl/min in 40 nl enrichment column (Agilent Technologies chip), with 0.1% formic acid as the eluent. The sample was then fractionated on a C18 reverse-phase capillary column (75 µm x 43 mm in the Agilent Technologies chip) at a

flow rate of 300 nl/min, with a linear gradient of eluent B (0.1% formic acid in acetonitrile) in A (0.1% formic acid) from 7 to 50% in 35 min. Elution was monitored on the mass spectrometers without any splitting device. Peptide analysis was performed using data-dependent acquisition of one MS scan (m/z range from 400 to 2000 Da/e) followed by MS/MS scans of the three most abundant ions in each MS scan. Dynamic exclusion was used to acquire a more complete survey of the peptides by automatic recognition and temporary exclusion (2 min) of ions from which definitive mass spectral data had previously been acquired. Moreover a permanent exclusion list of the most frequent peptide contaminants (keratins and trypsin peptides) was included in the acquisition method in order to focus the analyses of significant data.

2.6 Computational analysis

In this study we performed a BLAST search of PARP*Sso* sequence, on the web site http://blast.ncbi.nlm.nih.gov. We first searched all database with no "Entrez query" limit, and then we search a subset of the selected BLAST database for specific PARP domains and proteins (Figure 2-3). We used "blastp" algorithm with default general parameters.

2.7 Enzyme assays

ADP-ribosylating activity of crude and purified PARP*Sso* was assayed at 80°C in the presence of 0.64 mM [^{32}P]NAD^{+} (10000 cpm/nmol) according to Faraone Mennella *et al.*, 1998. Automodification reaction was monitored by precipitating proteins from the reaction mixture (62.5 μl) with ice-cold 20% TCA, freed of NAD^{+} with several 10% TCA washes, and the radioactivity present in the acid-insoluble material, was collected on a HAWP (0.45 μm, Millipore) filter and determined on a Beckman LS 1701 liquid scintillation spectrometer. One enzymatic unit was defined as the amount of enzyme catalyzing the incorporation, per min at 80°C, of 1 μmol of ADP-ribose into acid-insoluble material. Human sera and pure HPBP were assayed for mesophilic PARP activity at 25°C as previously described in Faraone Mennella *et al.*, 2003.

Alkaline phosphatase activity was assayed by monitoring the release of p-nitrophenol by hydrolysis of p-nitrophenyl phosphate (Pantazaki *et al.*, 2008). The reaction mixture consisted of 1 mM p-nitrophenyl phosphate and 50 mM KCl–NaOH buffer pH 12.3 in a final volume of 1 ml. The

reaction was initiated by adding 5 µl of sample preparation and the mixture was incubated at 70 °C (*Sulfolobus* proteins) or 37°C (human proteins). The reaction was followed by monitoring the absorbance increase at 405 nm. One enzyme unit represents the amount of enzyme hydrolysing 1 µmol of substrate per min under the aforementioned conditions.
As negative control the absorbance increase of a reaction mixture without enzymes was also measured. A commercial alkaline phosphatase from human placenta (type XXIV, Sigma-Aldrich, Milan, Italy) was the positive control.

2.8 Agarose gel electrophoresis

The fraction derived from the different extraction procedures were suspended in Loading Dye Solution (MBI Fermentas) and loaded on 1% agarose gel in TAE buffer (40 mM Tris, 0,1% Acetic acid, 1 mM EDTA), electrophoresed at 100 V , stained with 0.5 µg/ml of ethidium bromide and visualized in a UV transilluminator.

2.9 Fluorescence anisotropy

Fluorescence experiments were performed in Dr. Sandra Greive's lab (John Innes Centre, Norwich, UK). DNA oligonucleotides were chemically synthesized and purified by high pressure liquid chromatography (Integrated DNA Technologies, GB). The 45 bp oligo ("oligo ss-a"), tagged at 5'end with the fluorescent dye 5-6FAM, had the sequence 5'- /56-FAM/AT TTT AGC TAG TCG ACG TGG TCC ATA ATG CTT AAT CCC AAA TTA T -3'. The unlabeled oligo is shorter (half) than the tagged one and complement it starting from 3'-end (5'- ATA ATT TGG GAT TAA GCA TTA TGG ACC ACG TCG ACT AGC TAA AAT -3'). The mixture of the two oligos is indicated as "oligo ds-b". The anisotropy measurements were done with a LS 55 Fluorescence Spectrometer (Perkin Elmer) equipped with a Peltier cooler to control the sample temperature, in Sub-micro low head space cuvette (Starna) in a total volume of 13 µl, at 40 °C. Excitation and emission parameters were setted at 480 and 525 nm, respectively. Each oligo (50 nM) was titrated with PARP*Sso* in assay buffer (10 mM sodium phosphate, 5 mM EDTA, pH 8.0).

Anisotropy data were fitted to a "Ligand binding-1site" equation by using GraFit program. In the graphs the reported ΔA values (A_x-A_0) were obtained from the difference of anisotropy values in the presence (A_x) and in the absence (A_0) of increasing PARP*Sso*.

2.10 Nucleoid preparation

Nucleoid from *S. solfataricus* cells was isolated by a procedure described for *S. acidocaldarius* (Reddy T.R. and Suryanarayana T., 1989) with some modifications. Harvested cells (0.3 g) were suspended in 10 mM Tris-HCl, pH 7.5, 100 mM NaCl (1 ml) and were lysed by the addition of 10 mM Tris-HCl, pH 7.5, containing 1% Nonidet P-40, 2 mM spermindine-HCl, 10 mM Na_2EDTA (1 ml), cocktail of protease inhibitors (2μg/ml), 1 mM PMSF and incubated at 10 °C for 30 min. The lysate was centrifuged at 1000xg for 5 min. The clear viscous lysate was dissolved in 5% saccarose and layered on 15-50% discontinuous gradient in 10 mM Tris-HCl, pH 7.5, 3 mM $MgCl_2$, 1 mM PMSF and centrifuged at 10000xg for 16 hours. The gradient was fractioned by collecting 1 ml fractions from the top, dialyzed against water and analysed by SDS-PAGE and on agarose gel. Protein content was estimated by Bradford protein assay. Absorbance at 260 and 280 nm of the gradient fraction was also measured.

2.11 Lipid extraction and Thin Layer Chromatography (TLC)

For the detection of lipids, some main gradient fractions were subjected to lipid extraction according to Bligh, E. G., Dyer, W. J., 1959. Fractions (150 μl) were incubated with methanol (600 μl) and chloroform (300 μl) for 30 min at 37 °C. Then 420 μl water and 300 μl chloroform were added and the mixture was vortexed for 10 min at room temperature to mix the phases and centrifuged for 2 min at 2000xg for phase separation. The aqueous phase was removed. The lower chloroform phase was then completely evaporated and the lyophilized material was dissolved in chloroform/methanol (2:1, v/v; 10 μl) and loaded on TLC, silica gel plate (Merck chemicals, Milan, Italy). The system was eluted with chloroform/methanol/water (65:25:4, v/v). Staining with 0.5% Amido black 10B (Sigma Aldrich, Milan, Italy) in 1 M NaCl and 20% ethanol allowed to reveal lipids as blue spots (Plekhanov, A. Y., 1999).

2.12 Immunofluorescence microscopy

Fresh log-phase sulfolobal cells were fixed with 10% methanol and then, for cell wall permeabilization, they were suspended in 10 mM Tris/HCl pH 8.0 and incubated with proteinase K (20 µg/ml) at room temperature for 10 min according to some indications described in Teira *et al*., 2004. For immunofluorescence microscopy, permeabilized cells were suspended in PBS-2% BSA and incubated with anti PARP-1 Ab (Santa Cruz; 1:50) overnight at 4 °C. After washing with PBS, cells were incubated with the secondary antibody (Alexa Fluor 488 goat anti-rabbit IgG; Invitrogen, 1:200 in PBS) for 1 h, and finally washed in PBS. Human A375 melanoma cells were fixed with 4% formaldehyde, permeabilized with 0.5% triton, and analysed in the same way.

Live cells were stained with 4′,6′-diamidino-2-phenylindole (DAPI) (0.2 µg/ml; Molecular Probes) and FM 64 (5 µg/ml; Molecular Probes) for DNA and membrane detection, respectively (Sharp, M. D., Pogliano, K., 1999).

Microscopy images were carried out with an Olympus BX51 microscope with 100x UPlanF1and U-WIBA filter. Images were captured by analySIS software (SIS).

RESULTS

3.1 PARP*Sso* and DING proteins

3.1.1 PARP*Sso* amino acid sequence

The partial N-terminus amino acid sequence and some tryptic peptides of the homogeneous archaeal thermozyme showed that the N-terminus of PARP*Sso* presents DINGGGATL, which is characteristic of DING proteins (Di Maro *et al.*, 2009).
We performed by mass spectrometry a further analysis of the purified PARP*Sso* after separation on SDS-PAGE and digestion with trypsin of the Coomassie-stained protein band (Figure 6).

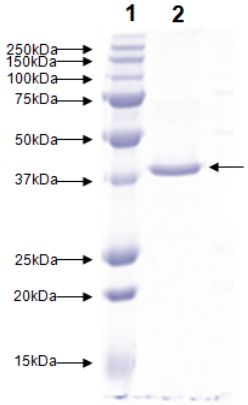

Figure 6: SDS-PAGE (12%) of purified PARP*Sso*.
Lane 1: Marker proteins; lane 2: PARP*Sso* (1.2 µg).

MALDIMSMS and LCMSMS analyses confirmed the previously sequenced regions and let to identify other peptides that align with DING protein sequences (human HPBP, 2CAP_A, and bacterial *Pflu*DING), Figure 7.

MH$^+$(mi) (MALDIMS)	Parent ion (LCESIMSMS)	PEPTIDE SEQUENCES (MALDI/MSMS and/or LC-ESI/MSMS)	Aminoacid number range
592.3		FLNAK	154-158
613.3		AFFTK	319-323
699.3		QPTWGK (con Gln->pyro-Glu)	78-83
716.3		QPTWGK	78-83
821.4		FVAGVSNK	47-54
1005.6	503.3	TGPITVVYR	133-141
1100.5		NVHWAGSDSK	55-64
1115.6		FVPLPDNWK	340-348
1143.5	572.3	AAFLTNDYTK	37-46
1171.6	586.4	DINGGGATLPQK	1-12
1201.6	601.6	TNVCcamDGI/LGRPI/L	367-377
1219.6		ITDWSGISGAGR	121-132
1314.6	657.9	SESSGTTELFTR	142-153
1412.7	707.0	LTATELSTYATNK	65-77
1521.01	761.1	GVMDAVNDTSVAEGR	194-208
1698.0		LIQVPSVATSVAIPFR	84-99
1736.9	868.6	SKGVMDAVNDTSVAEGR	192-208
1774.7		HFGDTNNNDDAITANR	324-339
1795.9	898.7	XXX(TD)NFVTASSALSIGK	349-366
1826.1	913.7	LIQVPSVATSVAIPFRK	84-100
2024.9	1013.2	SGANAVDLSVSELCcamGVFSGR	101-120
2111.0			65-83
2153.0		KSGANAVDLSVSELCGVFSGR	100-120
2188.0	1094.7	ITYMSPDFAASTLAGLDDATK	209-229
2204.0	1102.8	ITYMoxSPDFAASTLAGLDDATK	209-229
2358.2	1180.0	LYQTSGVLTAGFAPYIGVGSGNGK	13-36
2379.1			78-99 (con Gln->pyro-Glu)
2395.1			78-99
2514.3			209-232

Figure 7: MALDIMS (column one), and LC-ESIMSMS (column two) analyses. The sequences obtained by both analyses are reported in the third column.

Figure 8 shows the sequence obtained by integrating previous results (Di Maro *et al.*, 2009) with the new ones obtained by mass spectrometry, aligned with the sequences of other DING proteins.

```
PARPSso      -DINGGGATLPQKLYQTSGVLTAGFAPYIGVGSGNGKAAFLTNDYTKFVAGVSNKNVHWA 59
PfluDING     MDINGGGATLPQALYQTSGVLTAGFAQYIGVGSGNGKAAFLNNDYTKFQAGVTNKNVHWA 60
2CAP_A       -DIDGGGATLPEKLYLTPDVLTAGFAPYIGVGSGKGKIAFLENKYNQFGTDTT-KNVHWA 58
              **:*******: ** *.*******  *******:** *** *.*.:* :..: ******
                     §§                    §

PARPSso      GSDSKLTATELSTYATNKQPTWGKLIQVPSVATSVAIPFRKSGANAVDLSVSELCGVFSG 119
PfluDING     GSDSKLSATELSTYASAKQPTWGKLIQVPSVGTSVAIPFNKSGSAAVDLSVQELCGVFSG 120
2CAP_A       GSDSKLTATQLATYAADKEPGWGKLIQVPSVATSVAIPFRKAGANAVDLSVKELCGVFSG 118
             ******:**:*:***: *:* **********.*******.*.*: ******.********
               §

PARPSso      RITDWSGISGAGRTGPITVVYRSESSGTTELFTRFLNAKS------------------- 159
PfluDING     RINTWDGISGSGRTGPIVVVYRSESSGTTELFTRFLNAKCNAETGNFAVTTTFGTSFSGG 180
2CAP_A       RIADWSGITGAGRSGPIQVVYRAESSGTTELFTRFLNAKCTTQPGTFAVTTVFANSYSLG 178
             **  *.**:*:**:*** ****:****************.
                                  §   §§§

PARPSso      ------------KGVMDAVNDTSVAEGRITYMSPDFAASTLAGLDDATK---------- 196
PfluDING     LP-----AGAVAATGSQGVMTALAAGDGRITYMSPDFAAPTLAGLDDATKVAAVGKNVAT 235
2CAP_A       LTPLAGAVAAIGSDGVMAALNDTTVAEGRITYISPDFAAPTLAGLDDATKVAATGKGVVS 238
                           *   .:.  :..:*****:******.**********


PARPSso      -----GVSPAPSNVSDAIAQVLPP-----NDPSAPLDVTNPDDGVAGVQPYPDSGYPILG 246
PfluDING     --NTQGVSPAAANVSAAIGAVPVPAAADRSNPDAWVPVPGPDN-TAGVQPYPTSGYPILG 292
2CAP_A       GVAVEGKSPAAANVSAAISVVPLPAAADRGNPDVWVPVPGATT-GGGVVAYPDSGYPILG 297
                  * ***.:*** **. *  *     .:*.. : * ..    .** .** *******


PARPSso      FTNLIFS------------AFFTKHFGDTNNNDDAITANR-VPLPDNWKN-----FVTA 287
PfluDING     FTNLIFSQCYADATQTTQVRDFFTKHYGASNNNDAAITANAFVPLPTAWKATVRASFLTA 352
2CAP_A       FTDLIFSECYANATQTGQVRDFFTKHYGTSANDNAAIEANAFVPLPSNWKAAVRASFLTA 357
             **:****                 *****:* : *:: ** **  ****  **      *:**


PARPSso      SSALSIGKTNVCDGIGRPI-------- 306
PfluDING     SNALSIGNTNVCNGIGRPLLEHHHHHH 379
2CAP_A       SNALSIGNTNVCNGKGRPE-------- 376
             *.*****:****:* ***
```

Figure 8: Multialignment of PARP*Sso*, HPBP (2CAP_A), and *Pflu*DING by ClustalW program. The newly sequenced peptides are labeled in yellow. The conserved residues involved in phosphate-binding site in DING proteins are indicated (§).

At present 80% sequence of the sulfolobal protein is known with a fairly 90% similarity with DING proteins; the eight residues involved in phosphate-binding site of all DING proteins are conserved in PARP*Sso* sequence too.

BLAST search of PARP*Sso* sequence, integrated in the lacking peptides with those of HPBP sequence, with no "Entrez Query" limit, as expected, gave a list of DING and P-binding proteins with different scores and E-value depending on similarity percentages. This list did not include any PARP- or ADPRT- like sequence.

We performed a different BLAST search by indicating singularly as

"Entrez Query" key words related to PARP peculiar domains, namely PARP signature, macrodomain, WGR-, PAR binding domains, or single known PARP sequences from PARP1 to PARP18 (Figure 9).
This search was made in parallel for PARP*Sso*, HPBP, *Pflu*DING with similar results. Figure 9 shows the results for PARP*Sso*. Regions aligning with thermozyme are reported as a line that covers the corresponding DING sequence.

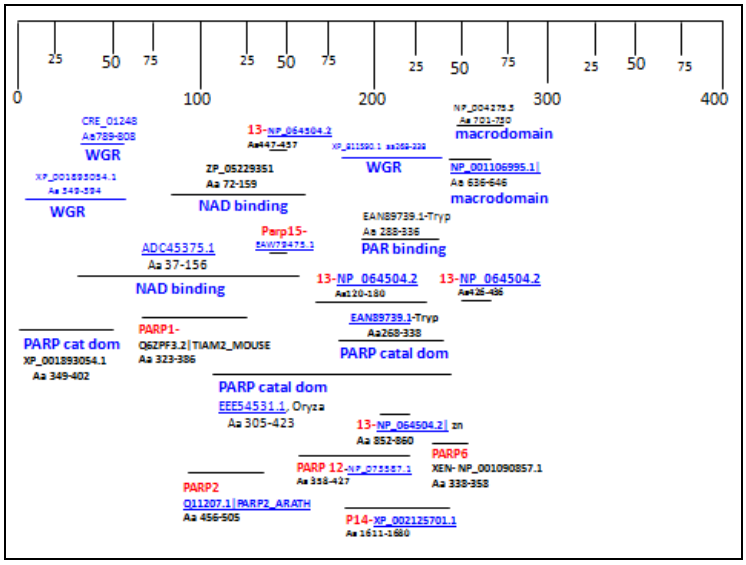

Figure 9: Blast results of "Entrez query" with PARP-related key words. PARP*Sso* sequence is indicated as black line on the top; numbers correspond to amino acid residues. Lines represent the PARP proteins regions aligning with PARP*Sso*. Accession number and amino acids aligned length of the protein resulting from the BLAST search are also reported. The domains are those of Figures 2-3.

Some amino acid motifs of PARP proteins matched with PARP*Sso*; several similarities were along the whole sequences and extended to different tipical PARP domains (catalytic domain, WGR, PAR binding and NAD binding domain, macrodomain).
A search for NAD-binding site was also performed among a series of resulting NAD dehydrogenases from different species; the two most significant ones were selected and shown in the Figure 9. It is worth noting that, despite the low similarity of aligned peptides, all derived PARP sequences were localized in correspondence of PARP*Sso* region spanning from about amino acid 100 to 300 (Figure 9).

3.1.2 Immunodetection of HPBP and PARP*Sso* with different antibodies

Considering the high structural similarity of PARP*Sso* with DING proteins, we performed immunoblotting analysis of the two purified proteins, PARP*Sso* and the human DING HPBP, with specific anti-PARP and anti-DING antibodies. DING proteins and antibodies were kindly provided by Ken Scott, New Zealand, and Eric Chabriere, France.
In Coomassie stained gel (Figure 10A) both HPBP (lane 1) and PARP*Sso* (lane 4) appeared highly purified with a single band at 38 kDa and >40 kDa respectively, compared to the starting samples, human serum (lane 2) and sulfolobal homogenate (lane 3).

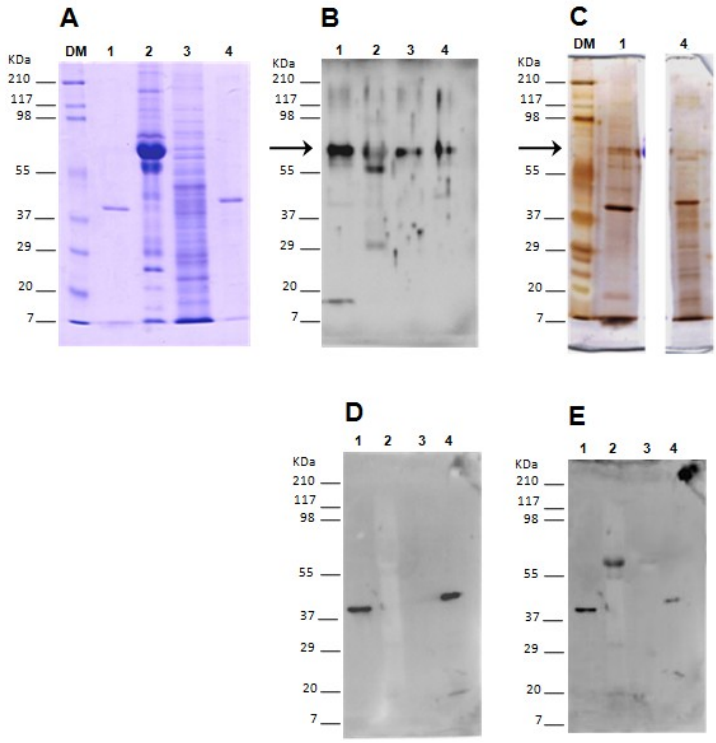

Figure 10: A) 12% SDS-PAGE of HPBP, lane 1; human serum, lane 2; sulfolobal homogenate, lane 3; purified PARP*Sso*, lane 4. Coomassie staining.
B) Immunoblotting with anti-PARP-CS Abs.
C) Silver staining of lanes 1 and 4 of gel in A.
D) Immunoblotting with anti-DING-Nterm Abs, after stripping of filter in B.
E) Immunoblotting with anti-*Pflu*DING Abs, after stripping of filter in D.

Their immunoblotting with commercial anti-PARP-CS Abs showed the same strong immunosignal between 55kDa and 98 kDa standard proteins (Figure 10B). This band was also evident in human serum (lane 2) and sulfolobal homogenate (lane 3). A second positive band corresponding to 55kDa was present in the human serum (lane 2). Much less intense was the immunoband at 38kDa-40kDa for all samples. Feeble bands above 117kDa were detected in all samples; a weak but net signal at 29 kDa was present in human serum (lane 2). For pure HPBP and PARP*Sso* (Figure 10A, lanes 1 and 4) silver staining of Coomassie-destained gel showed the presence in traces of bands corresponding to immunosignals between 55kDa and 98 kDa standard proteins (Figure 10C, lanes 1 and 4).
After stripping of the filter in Figure 10B and immunodetection with polyclonal anti DING-N-term Abs, a single, intense immunoband was localised only at about 40kDa, in correspondence of Coomassie stained pure HPBP and PARP*Sso* (Figure 10D, lanes 1, 4). It corresponded to the faint component identified by anti-PARP-CS Abs. No signals were present in serum and sulfolobal supernatant (Figure 10D, lanes 2, 3).
The filter was further stripped and incubated with polyclonal anti- *Pflu* DING (Figure 10B), and purified HPBP and PARP*Sso* responded as in Figure 10E (lanes 1, 4). In serum and sulfolobal homogenate only the 70 kDa signal appears at different intensities (Figure 10E, lines 2-3).

In a second experiment of SDS-PAGE and western blotting, both crude extracts (human sera, sulfolobal homogenate) and purified proteins (HPBP, PARP*Sso*) were analysed, by using anti-HPBP monoclonal and polyclonal antibodies.
As expected HPBP reacted with both monoclonal antibodies, giving an intense band at 40 kDa (Figure 11A, lane 1); a faint signal is present only for PARP*Sso* (Figure 11A, lane 2) and for human serum (Figure 11A, lane 4). After further stripping and polyclonal anti-HPBP*poliC* immunoblotting, both the purified proteins (HPBP and PARP*Sso*) reacted with a net signal close to 40kDa (Figure 11C, lanes 1, 2).

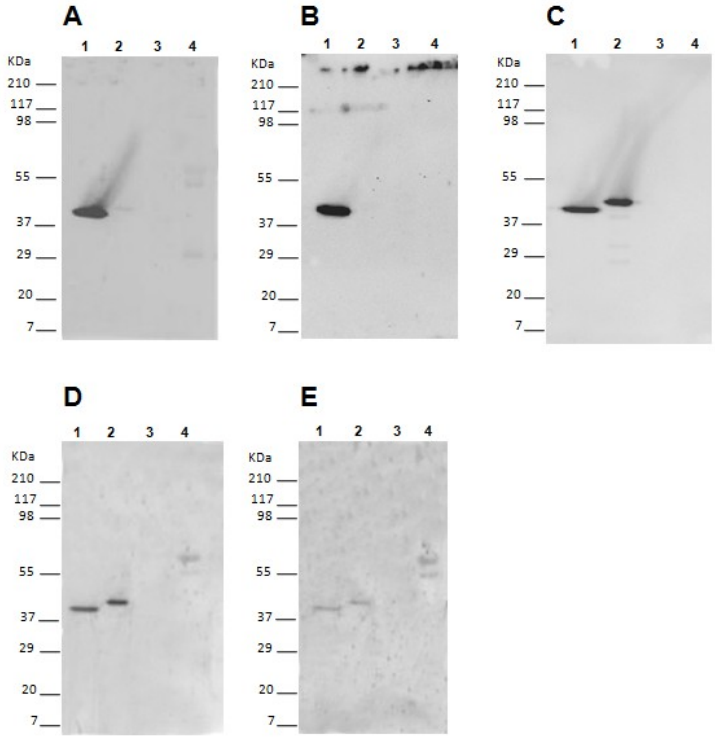

Figure 11: Immunoblotting analyses with monoclonal and policlonal anti-HPBP Abs, and with anti-PAR Abs.
Lane 1: HPBP; lane 2: PARP*Sso*; lane 3: sulfolobal homogenate; lane 4: human serum. Immunoblotting with:
A) monoclonal anti-HPBP 4D7 Abs.
B) monoclonal anti-HPBP 8H6 Abs, after stripping of filter in A.
C) policlonal anti-HPBP poliC, after stripping of filter in B.
D) anti-PAR Abs, after stripping of filter in C.
E) anti-PAR Abs, after stripping and alkaline incubation of filter in D.

3.1.3 Cross-reactivity of HPBP and PARP*Sso* with anti-PAR antibodies

Due the occurrence in *S. solfataricus* of endogenously automodified PARP*Sso*, that can be detected by immunoblotting with anti-PAR antibodies, the filter of Figure 11C was stripped again and analysed with anti-PAR polyclonal antibodies. Beside the two purified proteins, showing an immunoprofile overlapping that of Figure 11C, in the lane of serum two immunosignal between 55kDa and 98 kDa appeared (Figure 11D, lane 4). The slow migrating band was predominant.

In order to get evidence that the immunosignal with anti-PAR could be due to the presence of authentic poly-ADP-ribose, the stripped filter was incubated overnight under alkaline conditions. Alkaline medium detaches PAR from acceptor proteins, converting the latter in the unmodified form. Alkali-incubated filter was re-analysed with anti-PAR antibodies. The signals of Figure 11D were weakned, indicating that alkali had removed some bound poly-ADP-ribose (Figure 11E).

3.1.4 Enzymatic activities of HPBP and PARP*Sso*

The two purified proteins were assayed for ADP-ribosylating activity and gave the results reported in Table 2. PARP*Sso* was about 35 times more active than HPBP. Neverthless, the specific activity of the latter was comparable to that of rat testis crude nuclei, known to be particularly rich of PARPs. Eight different human sera collected at the transfusional centre were assayed. Although the activity measured was very low, radioactivity incorporation, expressed as mUnits/mg protein, was comparable for all sera.

TABLE 2 – ADP-ribosylating activity of HPBP and PARP*Sso*

Sample	mU/ml	mU/mg
Rat testis nuclei[1]	14 ± 2.2	0.7 ± 0.25
DNase supernatant[2]	4.5 ± 1.1	0.3 ± 0.07
Human sera[3]	0.17 ± 0.06	0.009 ± 0.003
PARP*Sso*[4]	16.7 ± 4.0	42 ± 5.0
HPBP[5]	0.25 ± 0.02	1.19 ± 0.07

[1]Mean value (MV) of 6 nuclei preparations from different adult male rats, in duplicate. [2]MV of three different DNase supernatants, in duplicate. [3]MV of 8 different human sera, in duplicate. [4]MV of 3 preparations of purified PARP*Sso*, in duplicate. [5]Triplicate assay on a single HPBP preparation.

As phosphate binding proteins, a presumable alkaline phosphatase activity was hypothesized for pure HPBP and PARP*Sso*. Figure 12 shows

the results for this assay. Compared to HPBP, the rate of absorbance increase was about three fold higher for PARP*Sso*.

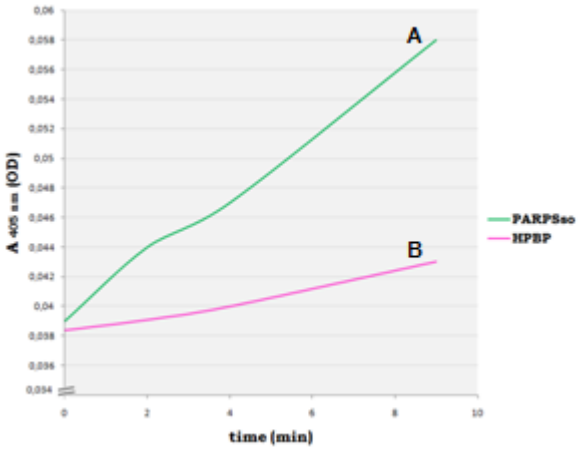

Figure 12: Reaction rates of PARP*Sso* (A) and HPBP (B) phosphatase activity. 2 µg enzyme/assay at 1 mM substrate**.**

Table 3 shows the corresponding specific activities, in comparison with phosphatase activity determined for DING protein from *Thermus thermophilus* (Pantazaki *et al.*, 2008). As a positive control commercial alkaline phosphatase from human placenta was used. The highest activity was measured for human placenta, close to that of *Thermus* enzyme. Much lower were the activities for HPBP and PARP*Sso*.

TABLE 3: Alkaline phosphatase activity of HPBP and PARP*Sso*

Sample	U/mg
PARP*Sso**	1.75
HPBP*	0.50
Human placenta phosphatase*	53.0
DING Phosphatase *from T. thermophilus* °°	54.0

*Mean value of a triplicate assay per sample; SD<5% ;
°°From Pantazaki *et al*., 2008.

3.2 Cell content and intracellular distribution of PARP*Sso*

Two main questions of the research on PARP*Sso* raised: its cellular content and its localization in intact cells.
In the laboratory where this thesis work has been developed, biochemical and structural properties of PARP*Sso* have been defined by analysing a pure protein purified from a crude homogenate. This sample, provided by the Fermentation service laboratory of ICMIB (CNR, Naples), was obtained from wet cells ground with glass beads and centrifugation as described in Faraone Mennella *et al.*, 1995. As this procedure allowed to solubilize fairly 50% of the whole protein content, one objective of this thesis was to determine the exact amount and intracellular distribution of the thermozyme starting from a whole cell culture.

3.2.1 Analysis of ADP-ribosylating activity in *S. solfataricus* cells at different growth phases

S. solfataricus cells were grown on complex (yeast) and minimum (glucose) medium and collected at exponential and stationary growth phases. After removing the growth medium by centrifugation, the pelleted cells (1 $O.D._{600}$), have been resuspended as described in Materials and Methods (§ 2.2) and tested for ADP-ribosylating activity (Table 4). PARP*Sso* activity was normalized to 1 O.D.

TABLE 4: ADP-ribosylating activity of lysed sulfolobal cells grown on yeast (Y) or glucose (G) medium at exponential (E) and stationary (S) phases.

CELLS	mU (10^{-2})/ $O.D._{600}$
CYE	3.5 ± 0.2
CYS	2.0 ± 0.3
CGE	3.8 ± 0.8
CGS	2.9 ± 0.6

The results indicate there is an inverse correlation between the growth phases and enzyme levels, with a decrease of enzyme activity from exponential phase to stationary one, for both Y and G media. These data

are in line with the reported ones for crude homogenate used in the past (Faraone Mennella *et al.*, 1995).

3.2.2 SDS-PAGE of sulfolobal cell lysates at different growth phases and extraction procedures

The sulfolobal cells, grown on complex and minimun medium were analysed on SDS-PAGE. The Coomassie-stained gel shows similar protein heterogeneity in all samples, except for CYS, where some bands are missed (Figure 13A). Anti-PARP antibodies (Abs) gave a main immunopositivity (less evident in CYS sample) at about 70 kDa for all samples and very weak signals at about 40 kDa, expecially for CGS. Some signals at low molecular weights are in CYS (Figure 13B).

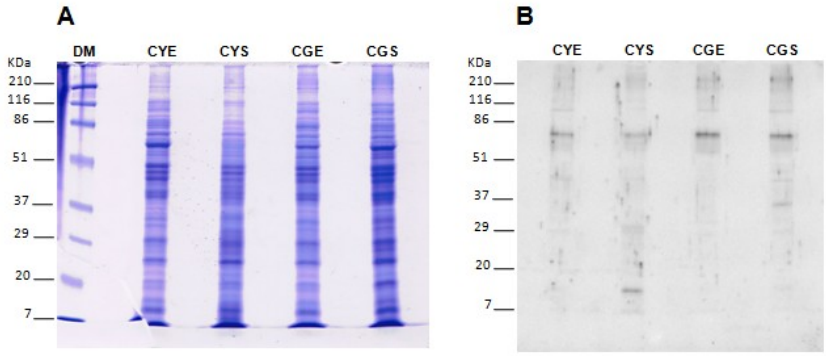

Figure 13: Analysis of total lysate of *S. solfatricus* cells (C) grown on yeast (Y) and glucose (G) medium at exponential (E) and stationary (S) growth phases. A) SDS-PAGE (12%), Coomassie staining; B) Immunoblotting analysis with anti-PARP-CS Abs.

Following this lysis procedure PARP*Sso* was detected as a band at high molecular weight rather than as 46.5 kDa protein. In order to study whether this form might be an artifact of the lysis procedure, and might be reverted to the 46.5 kDa protein, various extraction procedures from a whole cell culture on yeast medium at stationary phase were performed. The different protocols considered the new structural finding that indicate PARP*Sso* to be a DING protein, and that some other DING proteins are membrane bound.

Procedure 1

The pelleted cells were resuspended in lysis buffer, sonicated and centrifuged to separate the first soluble fraction (FS) from pellet (P1). Two successive extractions of pellets (MM) produced a ”Fraction with Medium Solubility (FMS)” and an ”Insoluble fraction” (FI), obtained with detergent treatment. The residual pellet was called (P3). This procedure is usually applied to separate cytoplasmic proteins (FS) from extrinsic membrane proteins (FMS) and intrinsic proteins (FI). The final pellet (P3) contains insoluble, proteinaceous material.
In Table 5 ADP-ribosylating activity values of PARP*Sso* in the various extracts (L, FS, FMS, FI) and in the pellet (P3) are reported. 11% of total activity (16.4 mU) is in FS, FMS, FI; about 42% is still associated with pellet. The latter activity might be understimated as for pellet it was difficult to quantify enzyme content.

TABLE 5: ADP-ribosylating activity of PARP*Sso* in different fractions

Fraction	Tot mg	Tot mU	mU/mg
Lysate (L)	202	16.4	0.08
FS	7.5	0.2	0.03
FMS	10	0.6	0.06
FI	18.8	1.0	0.05
P3	n.d.	7.0	n.d.

The assays were performed in duplicate, with SD ≤ 5%.

Protein extracts and pellet were analysed by SDS-PAGE followed by immunoblotting with anti PARP-CS Abs (Figure 14). Despite protein patterns are heterogeneous for all the extracts (FS, FMS, FI) and smearing in pellet 3, (Figure 14A), the immunosignal with anti-PARP-CS Abs is specific and is localized above the standard protein at 200 kDa; the signal is evident in L (lysate), very weak in FS and FMS, and more evident in FI. In line with activity results, most of the protein is still associated with the pellet, from low molecular weight to different aggregation forms (Figure 14B).

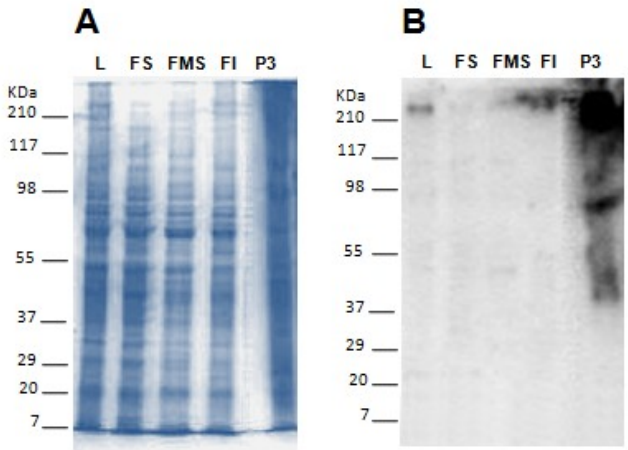

Figure 14: Analysis of protein extracts and pellet from procedure 1.
L: lysate; FS: Soluble Fraction; FMS: Fraction with Medium Solubility; FI: Insoluble Fraction; P3: residual pellet.
A) SDS-PAGE 12%, Coomassie staining.
B) Immunoblotting with anti-PARP-CS Abs.

These results indicate that the used extraction conditions produce probably an aggregated form of the enzyme, with respect to that present at about 70 kDa and observed in the analysis of the total cell lysate (Figure 14B). Only in the pellet, P3, other different forms at lower MW can be detected (Figure 14B).

Protein extraction from pellet 3

The association of most PARP*Sso* activity with pellet demonstrates that also in the past the enzyme recovery was not complete as the starting homogenate was already lacking in insoluble component (cell debris), removed by initial centrifugation.
In order to reduce the different immunosignals and to improve the recover from pellet 3, already derived from drastic extraction conditions, this fraction was divided in aliquots and treated, at 80 °C for 45 min, in the following conditions:

1- 1% Triton X-100
2- 1% SDS
3- 1% NP-40
4- 100 mM phosphate buffer, pH 7.5

Immunoblotting analysis with anti PARP-CS Abs after SDS-PAGE and western blotting of the extracts and remaining pellets, shows that, despite

the coomassie stained profiles indicate the solubilization of a lot of proteins (data not shown), in all the extracts the immunopositive signal is very weak and mostly localized at standard high MW proteins level (Figure 15A). The strongest signals are still associated to pellets. It is interesting to note that with non ionic detergents (Triton X-100 and NP-40) and phosphate buffer, there are more forms of the enzyme in the pellets, mainly the one at higher MW. Only SDS treatment seems to stabilize the form at about 70 kDa (Figure 15A).

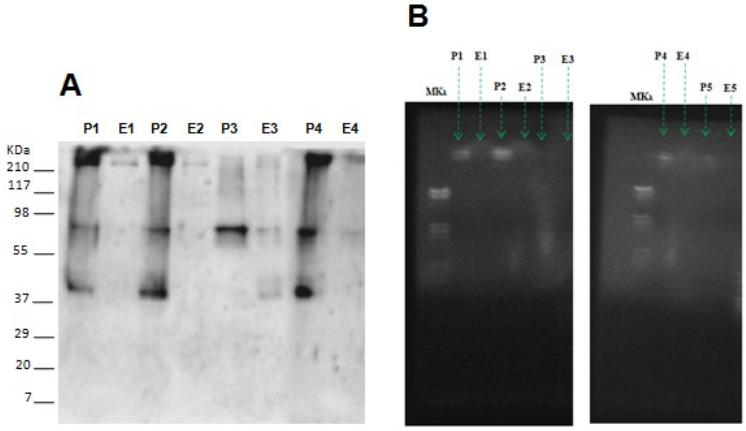

Figure 15: Analysis of the extracts (E) and remaining pellets (P) after treatment of the previous P3 in different conditions.
1: 1% Triton X-100; 2: 1% SDS; 3: 1% NP-40; 4: 100 mM phosphate buffer, pH 7.5. A) Immunoblotting with anti-PARP-CS Abs. B) 0.7% Agarose gel.

The analysis of the same samples on agarose gel indicates that in the pellet and in the extract after SDS treatment short fragments of DNA are present, compared to other pellets (P1, P2, P4) where DNA has larger size (Figure 15B).
Considering that PARP*Sso* interacts with endogenous DNA and that previously, enzyme solubilization was favoured by DNase digestion we performed a new protocol by adding DNase digestion step after lysis by sonication, and in the last step we utilized the best extraction, with 1% SDS, just tested before.

Procedure 2

Table 6 reports the activity values detected in the fractions obtained with procedure 2.

By comparing procedure 1 and 2, DNase I digestion is able to solubilize most of thermozyme already in the first, most soluble fraction. In fact, 50% is already present in FS_{DNase} and a further 20% in FI_{DNase}. The acid treatment utilized to have the FMS_{DNase} is probable responsible of the low activity of this fraction.

TABLE 6: ADP-ribosylating activity of PARP*Sso* in different fractions after DNase digestion

Fraction	Tot mg	Tot mU	mU/mg
Lysate $(L)_{DNase}$	130	30	0.23
FS_{DNase}	100	15	0.15
FMS_{DNase}	12	1.56	0.13
FI_{DNase}	11	6.5	0.56
$P3_{DNase}$	n.d.	5.8	n.d.

The assays were performed in duplicate, with SD ≤ 5%.

The samples of Table 6 were analysed by SDS-PAGE and immunoblotting as described before. An immunopositive signal is distributed in all fractions, either at high or low solubility (Figure 16B). In the pellet P3 and in FI_{DNase} it appears as a double band at about 70 kDa; some signals corresponding to aggregated forms are also present.

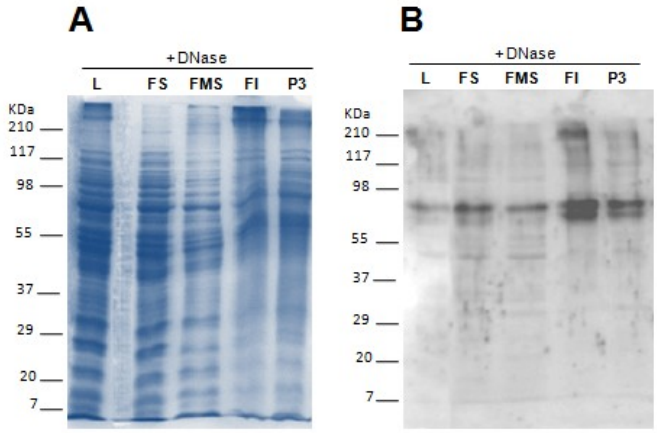

Figure 16: Analysis of protein extracts and pellet from procedure 2.
L: lysate; FS: Soluble Fraction; FMS: Fraction with Medium Solubility; FI: Insoluble Fraction; P3: residual pellet.
A) SDS-PAGE 12%, Coomassie staining.
B) Immunoblotting with anti-PARP-CS Abs.

Agarose gel electrophoresis of fractions from procedure 1 and 2

In absence of DNase treatment (procedure 1), in the lysate the DNA is mostly intact, except for small fragments probably due to the sonication effect; in the pellet the pattern is comparable, whereas in the extracts small DNA fragments are present (Figure 17A). After DNase digestion (procedure 2), cell lysate show DNA fragments with different size distributed up to the gel region corresponding to low MW fragments (Figure 17B). In FS_{DNase} smaller fragments are evident, whereas in FMS_{DNase} the fluorescence signal cover a middle gel region. The FI_{DNase} fraction is enriched in a band at about 1000 kbp, and in the pellet $P3_{DNase}$ there are DNA fragments with different sizes.

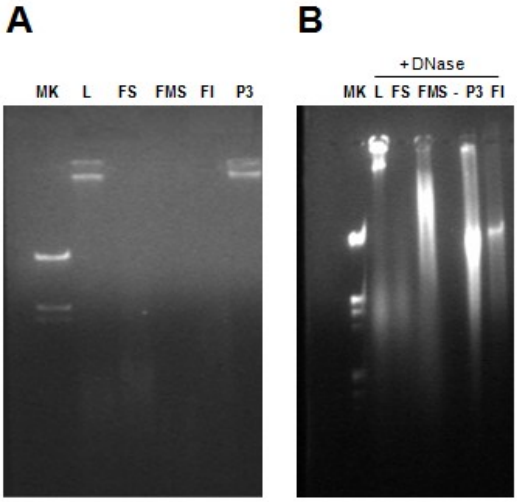

Figure 17: 1% Agarose gel analysis of the extracts and pellet from procedure 1 and procedure 2 (+ DNase I digestion).

Pellet extraction with organic solvent

The pellet $P3_{DNase}$ was subjected to butanolic extraction. The SDS-PAGE and immunoblotting analysis indicate that the protein is present in the organic phase, water phase and interphase (Figure 18A). The presence of the protein also in the organic phase, to which correspond a weak protein pattern (data not shown), suggests a very selective extraction of the enzyme, probably in association with apolar components such as membrane lipid. The DNA content analysis shows the co-presence of the enzyme with DNA (Figure 18B).

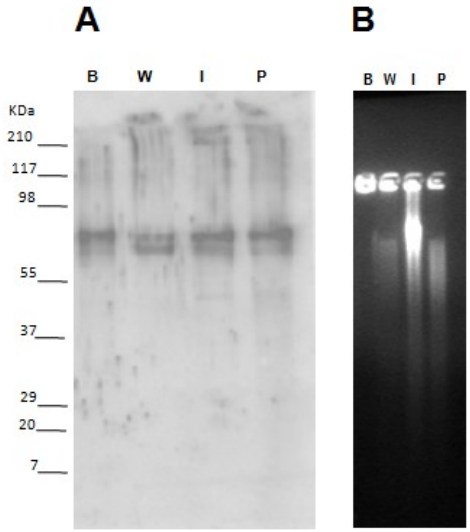

Figure 18: Analysis of fractions obtained from butanolic extraction of pellet $P3_{DNase}$.
B: butanolic phase; W: water phase; I: interphase; P: pellet
A) Immunoblotting with anti-PARP-CS Abs.
B) 1% Agarose gel.

3.3 Interaction of PARP*Sso* with DNA

The results obtained from the new extraction approaches raised some new questions about intracellular localization of thermozyme. Its resistance to detergents and distribution in both aqueous and organic fractions allowed to hypothesize that PARP*Sso* is probably interacting with membrane. On the other hand the enzyme had been found to bind DNA (Faraone Mennella *et al.*, 2002), and, in the present study, sulfolobal DNA is associated with PARP*Sso* almost in all fractions obtained with the new procedures.
Therefore, further researches were addressed to get further evidences of PARP*Sso*/DNA interaction and to explain the widespread distribution of DNA even in those fractions where PARP*Sso* seems to be associated with membrane lipids, being soluble in organic solvent.
Three experimental approaches were used: 1- PARP*Sso*/DNA interaction was tested in sensible reconstitution experiments with purified PARP*Sso* and fluorescent ss- and ds-oligonucleotides of different structures; 2- sulfolobal nucleoid was prepared by centrifugation of cell lysate on sucrose gradient; 3- fluorescent microscopy analysis was performed with intact cells to immunolocalize PARP*Sso* intracellularly.

3.3.1 Fluorescence binding assay

In this study we used a sensitive fluorescence anisotropy method to characterize the interaction of PARP*Sso* with different types of single and double stranded oligonucleotides.
In these preliminary experiments the 5'-FAM labeled ssDNA oligonucleotide is 45 bp with low GC percent according to the sulfolobal genome characteristics. The addition of PARP*Sso* led to an increase in fluorescence anisotropy (Figure 19A), and when data were fitted to a Ligand binding-1 site equation (Materials and Methods, § 2.9), yielded a dissociation equilibrium constant of 3.7 μM.

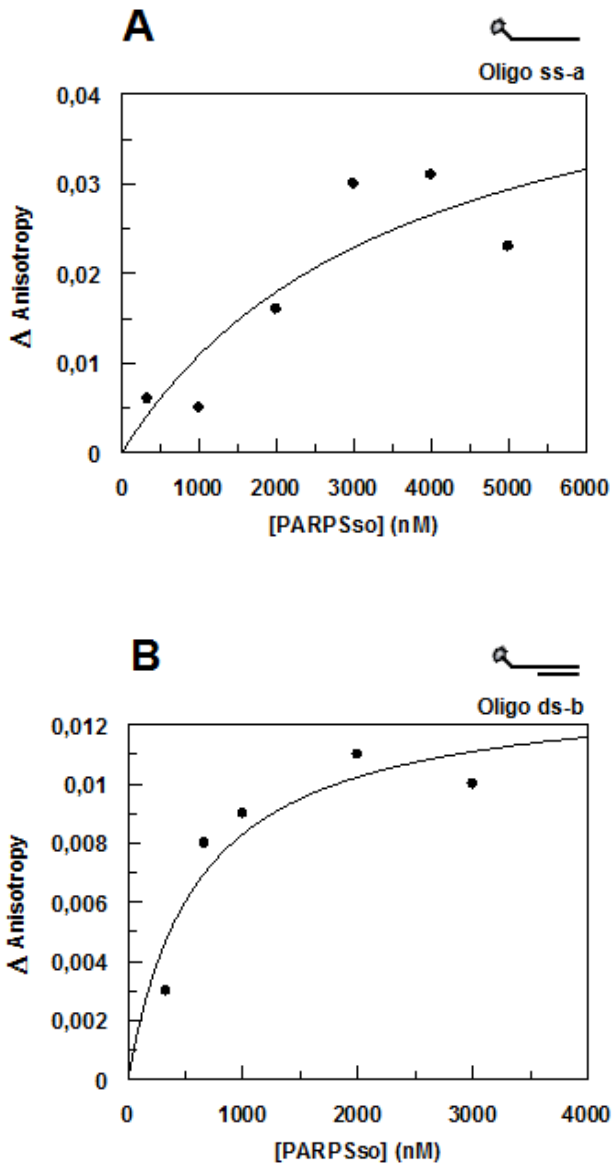

Figure 19: Anisotropy curves for binding of PARP*Sso* to DNA oligos. Fluorescence anisotropy was reported as ΔAnisotropy values ($\Delta A = A - A_0$; Materials and Methods § 2.9)
Titration of PARP*Sso* with 50 nM of A) 5'-FAM labeled single strand oligo: oligo ss-a; B) 5'-FAM labeled double strand oligo: oligo ds-b.

When fluorescence anisotropy titration with 50 nM "oligo ds-b" (Figure 19B) was performed with PARP*Sso*, we observed an high affinity binding to DNA corresponding to K_d value of 0.6 μM, about 6 times lower than the previous one. This means that affinity of PARP*Sso* for "oligo ds-b" is higher than that for single strand oligos.
No significant changes in anisotropy were observed when 50 nM of different dsDNA oligos (nicked and gapped dsDNA) were titrated with PARP*Sso* (data not shown), indicating that, under the experimental conditions used, no strong interaction occurs between these structures.

3.3.2 Nucleoid preparation

In order to study PARP*Sso*-DNA interaction with respect to own genomic DNA, the archaebacterial nucleoid from *S. solfataricus* cells was isolated. Suspension of cell lysate in 5% sucrose before layering onto sucrose gradient, allowed to avoid trapping of heavy material (chromatin) on the top of the gradient. DNA and protein content of the collected fractions were estimated by monitoring absorbance at 260 and 280 nm respectively (figure 20A). The two profiles were almost overlapping, with high absorbance peaks corresponding to low percent of sucrose gradient, followed by an intermediate region with small peaks and an increase of absorbance towards the bottom of the gradient (Figure 20A).

According to UV absorbance profiles, the fractions corresponding to low percent of sucrose gradient (top) are enriched of DNA, as revealed by their analysis on agarose gel (Figure 20B). At the top of the gradient (15-20% sucrose; fractions 1-8), DNA with higher electrophoretic mobility was localized, while at 45-50% sucrose, (fractions 28-35) the fluorescence signal was retained at the top of the gel (larger DNA), Figure 20B.

As revealed by immunoblotting with anti-PARP-CS antibodies, in the chromatin fractions at top PARP*Sso* appeared also in the low molecular weight form at about 40 kDa, associated with high and medium mobility DNA (Figure 20C).

In correspondence of low electrophoretic mobility DNA (towards the bottom of the gradient), a main signal at about 70kDa was predominant (Figure 20C).

In the fractions 14-27, corresponding to the middle gradient region, traces of DNA (Figure 20B) and PARP*Sso* (data not shown) were detectable.

The specific association of DNA and thermozyme with both low (top) and high (bottom) sucrose gradient, but not in the middle of it, suggests a non random distribution of chromatin fractions that would be expected to localize only at the highest sucrose percent.

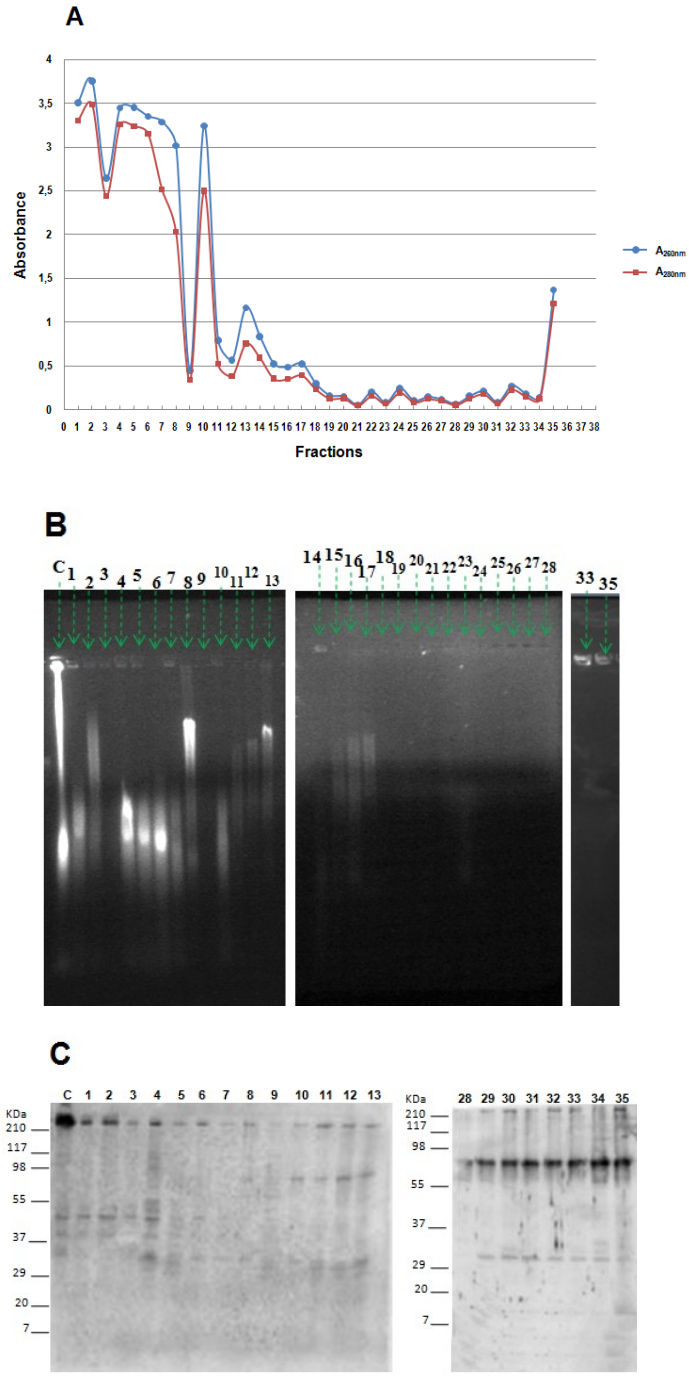

Figure 20: A) Sucrose gradient profile of nucleoid from *S. solfataricus* lysate. The 1 ml fractions were analyzed for UV absorption, at 260nm (blu line) and at 280nm (red line); B) 0.7% Agarose analysis of gradient fractions; C) Immunoblotting with anti-PARP-CS Abs of gradient fractions after SDS-PAGE 12%.

In order to understand whether and where the gradient fractions could contain membrane lipids, present in the cell lysate, we chose to analyse some fractions at different gradient percentage. Fractions 2, 5, 8, 10, 13, 22, 32, 35 were separated on TLC and stained with amido Black. The blue color indicated the presence of lipids in all the analysed fractions (Figure 21). Lipids were expected to be present in the upper gradient fractions, because membranes, lighter than chromatin, are retained at low sucrose percent. As opposite it is rather unusual to find lipids associated with heavy chromatin at bottom of the gradient.

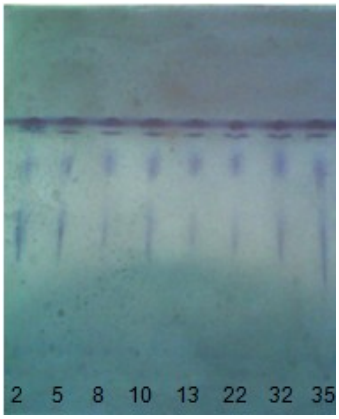

Figure 21: Separation of some main gradient fractions via thin layer chromatography. Visualization of lipids was performed by using 0.5% amido Black; numbers correspond to the analyzed gradient fractions after lipid extraction procedure.

3.4 Intracellular localization of PARP*Sso*

In order to investigate the intracellular localization of PARP*Sso* and its relationship with cell components, we carried out fluorescence light microscopy experiments on *S. solfataricus* cells, fixed with 100% methanol, by using DNA staining with DAPI, membrane staining with FM64, and in parallel anti-PARP-CS antibodies.

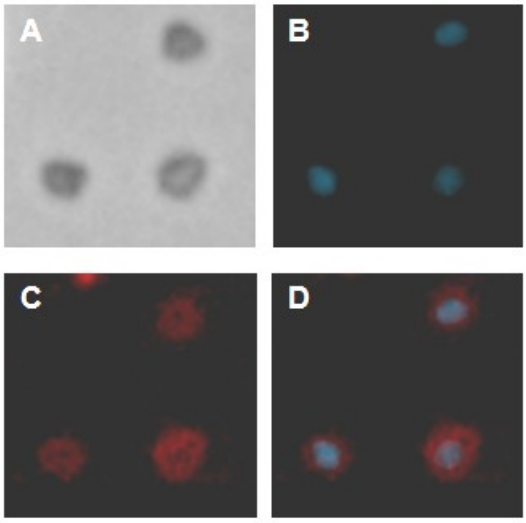

Figure 22: Epifluorescence microphotographs of *S. solfataricus* cells.
A) Phase contrast image; B) DAPI-stained DNA (blue); C) FM64 staining of cell membrane (red); D) Merged image of DAPI- and FM64-stained cells.

The blue color of DNA is centered in the cell (Figure 22, panel B), whereas all around, along the edge of the cell the membrane is detected in red (Figure 22, panel C). The merged image of DAPI- and FM64-stained cells is shown in panel D of the same figure.
The fluorescence detection with anti-PARP-CS Abs shows a distribution of the enzyme that outlines the perimeter of the cells (Figure 23). This first result is indicative of membrane localization of PARP*Sso*.
Human A375 melanoma cell line was used as positive control, and compared with the membrane staining by FM-64, the immunofluorescence with anti-PARP-CS antibody indicates PARP-1 accumulates in the nucleus (Figure 24).
Moreover, as a control of the specificity of the anti-PARP-CS antibody, we also verified the absence of detectable signal in *E. coli* cells (Figure 24).

***S. solfataricus* cells**

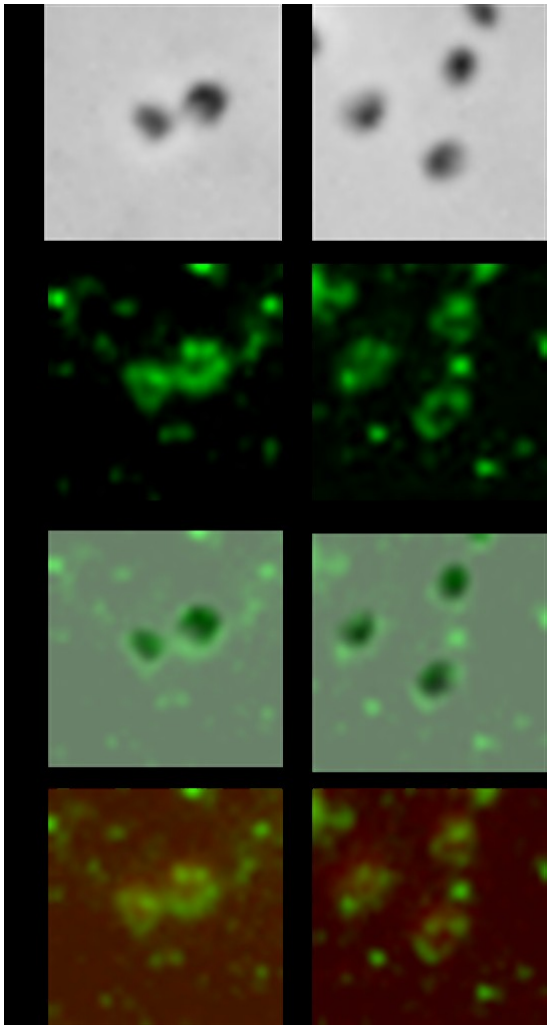

Figure 23: Immunolocalization of PARP*Sso* in sulfolobal cells
A) Phase contrast image; B) Localization of PARP*Sso* with the specific anti-PARP-CS antibody: secondary antibody coupled to Alexa Fluor 488 (green); C) Merge of a phase contrast image and an immunofluorescence image of *S. solfataricus* cells; D) Merge of stained membrane image (red) and the immunolocalization with anti-PARP-CS antibody (green).

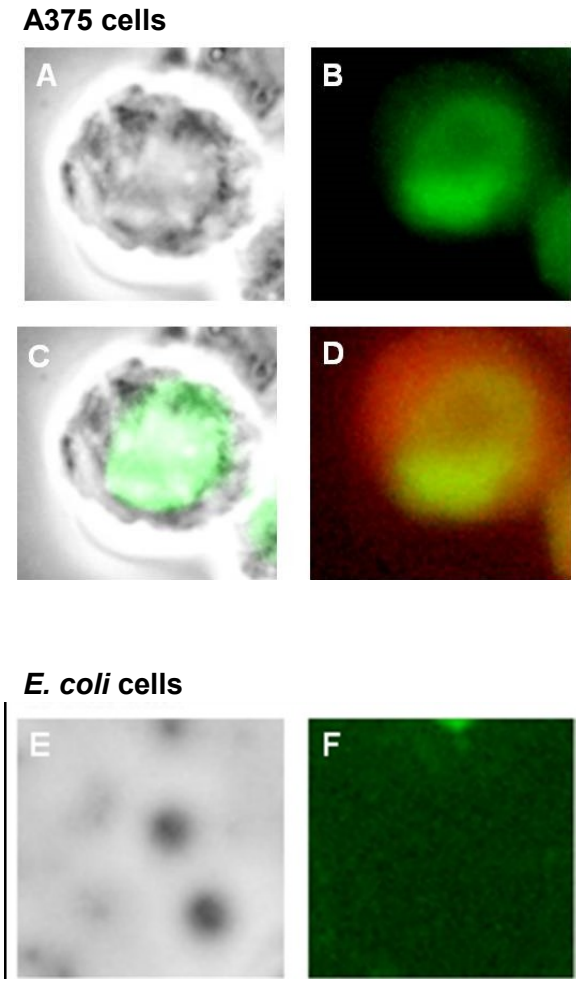

Figure 24: Immunofluorescence microscopy with anti-PARP-CS Abs in human A375 melanoma cells and *E. coli* cells.
A375 cells: A) Phase contrast image; B) immunolocalization of PARP-1 with the specific anti-PARP-CS antibody; secondary antibody coupled to Alexa Fluor 488 (green). C) merge of phase contrast image and immunofluorescence image. D) merge of FM64 stained membrane image (red) and immunofluorescence signal.
E. coli cells: E) Phase contrast image; F) immunofluorescence analysis with anti PARP-CS antibody.

4. DISCUSSION/CONCLUSIONS

Since its discovery in *S. solfataricus*, PARP*Sso* was object of a hard criticism as the sulfolobal genome did not include any gene sequence corresponding to classic PARPs. Neverthless, biochemical, kinetic and immunological data, together with characterization of reaction products allowed to define it as a PARP-like enzyme, although with specific features linked to its thermophilic nature.

The partially sequenced thermozyme overlaps the sequences of a class of proteins rather different than PARPs, the DING proteins. It is worth noting that the present partial amino acid sequence of PARP*Sso* (46.5 kDa) matches that of HPBP (38 kDa), the human serum DING protein, whose sequence is now complete.

In the present work, in order to understand the relationship between biochemical and structural data about PARP*Sso* and to know whether its behaviour is general for DINGs, crossing immunochemical and enzymatic analyses were undertaken with both human and sulfolobal proteins.

As a matter of the fact, HPBP and PARP*Sso* have been demonstrated to be able to cross react with polyclonal either PARP and DING antibodies, the latter directed against bacterial or eukaryotic DINGs.

An hypothesis is that the antigenic ability of the two proteins towards anti-PARP catalytic site antibodies, may be a consequence of tertiary rather than primary structure similarity. Evidence raised by immunochemical results may be in line with this hypothesis. In fact, the main anti- PARP-CS immunosignal has a mobility relative to about 70 kDa, corresponding to a faint band detected by silver staining in both proteins, suggesting that antibodies recognized a more structured conformation than the 40 kDa one (Figure 10B, lanes 1-4).

It must be underlined that 40 kDa-larger precursors of HPBP have been described in literature, whereas a “dimeric” form of PARP*Sso* is observed after some mechanical treatments (sonication) of sulfolobal samples (crude extracts). The 46.5 kDa PARP*Sso* often changes into 70 kDa form, that is very stable under different treatments (De Maio *et al.*, 2010).

The fact that polyclonal anti-PARP-CS recognize preferentially the 70 kDa in both samples lets to hypothesize that a different epitope raises from dimerization of purified proteins with a higher antigenic ability.

Anti-*Pflu*DING antibodies recognize this band only in sera and sulfolobal extract, but they react preferentially with monomer of HPBP and PARP*Sso*. Polyclonal anti-DING-N-terminal antibodies reveal only the monomers of the two purified proteins at about 40 kDa.

Focusing on the purified proteins, and considering that the presence of

precursors and/or contaminants can be excluded on the basis of amino acid sequence studies (a single N-terminus detected, peptide maps overlapping), the different behaviours of anti-PARP and anti-DING polyclonal antibodies suggest that they recognize one of the possible protein conformations.
As expected, monoclonal antibodies are rather specific for 38 kDa HPBP; with one of the two monoclonal antibodies, a weak signal for PARP*Sso* at about 40 kDa is also evident.
It is worth noting that both proteins reacts with anti-PAR antibodies. They are fully reactive with monomers of HPBP and PARP*Sso*, indicating that both proteins are endogenously modified with polymer.
The reactivity towards anti-PAR Abs allows to draw an hypothesis about the different cross–reactivity of the other analysed antibodies. The dimeric form of the two proteins presumably masks the presence of poly-ADP-ribose, since anti-PAR do not recognize the 70kDa band. On the other hand the presence of PAR might reduce the antigenicity of monomeric HPBP and PARP*Sso* towards anti-PARP-CS and produce the weak response observed.
Anti-human N-terminus and anti-*Pflu*DING Abs have a high cross reactivity for both HPBP and PARP*Sso* at 40 kDa, as they recognize common structural regions, that might be masked in the high molecular weight forms of proteins. The only dimeric "signal", with anti-*Pflu*, is in serum, thus suggesting the presence of a DING precursor.
These results clearly show that HPBP and PARP*Sso* share a cross reactivity towards anti-DING, -PARP, -PAR antibodies, and beside the still partial amino acid sequence of PARP*Sso*, both proteins possess similar if not identical epitopes allowing to be recognized by all antibodies in either one (~40 kDa) or the other (>40 kDa) isoform. Functionally, they work as both PARP and alkaline phosphatase, although at different extents.
PARP*Sso* exhibits both activities higher than HPBP, and functions preferentially as ADP-ribosylating enzyme, with a specific activity 35 times that of HPBP. Phosphatase activity of PARP*Sso* was only 3 times higher than HPBP, although for both HPBP and PARP*Sso* it was very low as compared with *Thermus* and human placenta enzymes.

A main question raised with this work is the localization of PARP*Sso* within the cell. Its association with DNA was widely demonstrated in the past (Faraone Mennella *et al.*, 2002) and here it has been confirmed by anisotropy measure with fluorescent oligonucleotides. The new evidence from nucleoid preparation and fluorescent microscopy is that PARP*Sso*

interacts also with cell membrane.
A very recent paper reports that in sulfolobal cells the exosome, a RNA-processing protein complex**,** is membrane-bound, and that membrane is involved in the spatial organization of the nucleic acid (Roppelt *et al.*, 2010). Their results of nucleoid preparation and immunofluorescent microscopy are very similar to those we obtained from our experiments.
As the exosome proteins, PARP*Sso* is localized along the periphery of the cell and the immunofluorescence signal overlaps that of membrane staining. On this basis can PARP*Sso* be considered exclusively the bridge element between DNA and the cell membrane? Some of the presented results suggest that sometimes the thermozyme is still anchored to the membrane after all DNA is removed. Does this mean that the enzyme might exhibit also another function different from regulating DNA metabolism/organization? Further study is needed to answer this question.
In conclusion, what emerges from the present data is a common immunological and enzymatic behaviour of human and sulfolobal proteins. They have structural similarity, with a phosphate binding motif, that allows to predict the phosphatase activity, found at low, but comparable levels. What is difficult to explain is that they both seem to be structurally unrelated with the classic PARP family.
This question needs specific phylogenetic studies that go beyond the aim of this work. However we attempted an arbitrary computational approach to get evidence of any, even small, correlation of PARP*Sso* with PARP structure.
From BLAST and Prosite research towards all data bases, the available PARP*Sso* sequence, integrated for the lacking peptides with the corresponding ones of HPBP, gave alignments with other DINGs and phosphate-binding proteins, but not with PARPs or any ADP-ribosylating enzyme. Therefore, we restricted the search field by using key words related to typical PARP domain or corresponding to each known PARP (from PARP-1 to PARP-18). The results allowed to draw the scheme of Figure 9, suggesting that despite the low similarity of aligned peptides, all PARP sequence derived from BLAST are localized in a specific amino acid region of PARP*Sso*, spanning from the amino acid 100 to 300. Moreover, ahead of this sequence, there is a correspondence of PARP*Sso* with NAD binding sites of pyridinic dehydrogenases.
A re-evaluation of these data will be done in next studies, taking into account the alignment casuality and performing a systematic phylogenetic study, calculating the distances on the basis of possibly occurred mutations and of further experimental data.
Far from drawing definite conclusions we can hypothesize that DINGs

and PARPs originated as a single protein with different structural modules, that underwent different evolutive fates to produce in higher organisms two proteins structurally and functionally divergent.
As a matter of fact, in Archaea, simple prokaryotes with a simple proteome, it is frequent that an enzyme can exhibit various activities. PARP*Sso* shows to be a multifunctional enzyme with both PARP and DING properties. It is conceivable that during evolution, different modules developed: the DING one, in a structurally related, but probably functionally different protein (DING, HPBP), with a residual "trace" of PARP activity, whereas other module(s) in *S. solfataricus* became the starting point to generate a different kind of enzyme, namely PARP.
On this basis we feel to draw a bold hypothesis that the dichotomy of HPBP and PARP*Sso* might be explainable as a product of a divergent evolution towards ortologue proteins.

REFERENCES

Amé, J.C., Rolli, V., Schreiber, V., Niedergang, C., Apiou, F., Decker,P., S. Muller, T. Hoger, J. Menissier-de Murcia, de Murcia, G. (1999) PARP-2, A novel mammalian DNA damage-dependent poly(ADP-ribose) polymerase. J. Biol. Chem. 274, 17860–17868.

Amé, J.C., Spenlehauer, C., de Murcia, G., (2004) The PARP superfamily. Bioessays 26, 882–893.

Benjamin, R.C., Gill, D.M. (1980) ADP-ribosylation in mammalian cell ghosts. Dependence of poly(ADP-ribose) synthesis on strand breakage in DNA. J. Biol. Chem. 255, 10493–10501.

Berna A, Bernier F, Chabrière E, Perera T, Scott K. 2008. DING proteins; novel members of a prokaryotic phosphate-binding protein superfamily which extends into the eukaryotic kingdom. Int J Biochem Cell Biol 40: 170–179.

Berna, A., Bernier, F., Chabrie`re, E., Elias, M., Scott, K., Suh, A. (2009) For whom the bell tolls? DING proteins in health and disease. Cell. Mol. Life Sci. 66, 2205–2218

Berna, A., Bernier. F., Scott, K., Stuhlmuller, B. (2002) Ring up the curtain on DING proteins. FEBS Lett 524, 6–10

Berna, A., Scott, K., Chabrière, E., Bernier, F. (2009) The DING family of proteins: ubiquitous in eukaryotes, but where are the genes? Bioessays. 31, 570-80.
Biochem Biophys Res Commun. 389, 284–289.

Bligh, E.G., and Dyer, W.J. (1959) A rapid method of total lipid extraction and purification. Can. J. Med. Sci. 37, 911-917.

Castellano, S., Farina, B., Faraone-Mennella M.R. (2009) The ADP-ribosylation of *Sulfolobus solfataricus* Sso7 modulates protein/DNA interactions in vitro. FEBS Lett. 583, 1154-8.

Collombet, J.M., Elias, M., Gotthard, G., Four, E., Renault, F., Joffre, A., Baubichon, D., Rochu, D., Chabrière, E. (2010) Eukaryotic DING proteins are endogenous: an immunohistological study in mouse tissues. PLoS One 5(2):e9099.

Contreras-Martel, C., Carpentier, P., Morales, R., Renault, F., Chesne-Seck, M.L., et al. D'Amours, D., Desnoyers, S., D'Silva, I., Poirier, G.G. (1999) Poly(ADP-ribosyl)ation reactions in the regulation of nuclear functions. Biochem. J. 342, 249–268.

Darbinian-Sarkissian, N., Darbinyan, A., Otte, J., Radhakrishnan, S., Sawaya, B.E., Arzumanyan, A., Chipitsyna, G., Popov, Y., Rappaport, J., Amini, S., Khalili, K. (2006) p27SJ, a novel protein in St John's Wort, that suppresses expression of HIV-1 genome. Gene Ther 13, 288–295.

De Maio, A., Porzio, E., Romano, I., Nicolaus, B., Faraone Mennella, M.R. (2010) Purification of the poly-ADP-ribose polymerase - like thermozyme from the archaeon *Sulfolobus solfataricus*. Methods In Molecular Biology; ISSN: 1064-3745, p.1-25 *in press.*

De Rosa, M., Gambacorta, A., Bullock, J.D. (1975). Extremely thermophilic acidophilic bacteria convergent with *Sulfolobus acidocaldarius*. J. General Microbiology, 86, 156-164.

Desmarais, Y., Ménard, L., Lagueux, J., Poirier, G.G. (1991) Enzymological properties of poly(ADP-ribose)polymerase: characterization of automodification sites and NADase activity. Biochim Biophys Acta. 1078, 179–186.

Di Maro, A., De Maio, A., Castellano, S., Parente, A., Farina, B., Faraone-Mennella, M.R. (2009) The ADP-ribosylating thermozyme from *Sulfolobus solfataricus* is a DING protein. Biol Chem. 390, 27-30 .

El-Khamisy, S.F., Masutani, M., Suzuki, H., Caldecot K.W. (2003) A requirement for PARP-1 for the assembly or stability of XRCC1 nuclear foci at sites of oxidative DNA damage. Nucleic Acids Res. 31,5526-33.

Faraone-Mennella, M,R., De Lucia, F., De Maio, A., Gambacorta, A., Quesada, P., De Rosa, M., Nicolaus, B., Farina, B. (1995) ADP-ribosylation reactions in *Sulfolobus solfataricus*, a thermoacidophilic archaeon. Biochim Biophys Acta. 1246, 151-9.

Faraone-Mennella, M.R., De Luca, P., Giordano, A., Gambacorta, A., Nicolaus, B., Farina, B. (2002) High stability binding of poly(ADPribose) polymerase-like thermozyme from *S. solfataricus* with circular DNA. J.Cell. Biochem. 85, 158-166.

Faraone-Mennella, M.R., Farina, B. (1995) In the thermophilic archaeon *Sulfolobus solfataricus* a DNA-binding protein is in vitro (ADP-ribosyl)ated. Biochem. Biophys. Res Commun 208, 55-62.

Faraone-Mennella, M.R., Gambacorta, A., Nicolaus, B., Farina, B. (1998) Purification and biochemical characterization of a poly(ADP-ribose) polymerase-like enzyme from the thermophilic archaeon *Sulfolobus solfataricus*. Biochem. J. 335, 441-447.

Faraone-Mennella, M.R., Piccialli, G., De Luca, P., Castellano, S., Giordano, A., Rigano, D., De Napoli, L., Farina, B. (2002) Interaction of the ADP-ribosylating enzyme from the hyperthermophilic archaeon *S. solfataricus* with DNA and ss-oligo deoxy ribonucleotides. J Cell Biochem. 85, 146-57.

Faraone-Mennella, M.R., Roma, G., Farina, B. (2003) Active poly(ADPribose) metabolism in DNAase- and salt-resistant rat testis chromatin with high transcriptional activity/competence. J Cell Biochem 89, 688-697.

Ferro, A.M, Olivera, B.M., (1982) Poly(ADP-ribosylation) in vitro. Reaction parameters and enzyme mechanism, J. Biol. Chem. 257, 7808–7813.

Gambacorta, A., De Rosa, M., Lama, L., Nicolaus, B. (2004) Sulfolobales lipids: new solutions in the lipid's world Research Signpost, 37/661: 1-22.
Gene. Volume 146. 2, 209-213.

Hassa, P. O., and Hottiger, M. O. (2008) The diverse biological roles of mammalian PARPS, a small but powerful family of poly-ADP-ribose polymerases. Front. Biosci. 13, 3046–3082.

Hassa, P.O., Haenni, S.S., Elser, M., Hottiger, M.O. (2006). Nuclear ADP-Ribosylation reactions in Mammalian cells: where are we today and where are we going? Micr and Mol Biology Reviews 70, 789-829.

Hayashi, K., Tanaka, M., Shimada, T., Miwa, M., Sugimura, T. (1983) Size and shape of poly(ADP-ribose): examination by gel filtration, gel electrophoresis and electron microscopy, Biochem. Biophys. Res. Commun. 112, 102–107.

Hottiger, M.O., Hassa, P.O., Lüscher, B., Schüler H, Koch-Nolte, F. (2010) Toward a unified nomenclature for mammalian ADP-ribosyltransferases. Trends Biochem Sci. 35, 208-19.

Keeling, P.J., Doolittle, W.F. (1995) Archaea: narrowing the gap between prokaryotes and eukaryotes. Proc Natl Acad Sci U S A. 92, 5761–5764.

Kleine, H., Poreba, E., Lesniewicz, K., Hassa, P.O., Hottiger, M.O., Litchfield, D.W., Shilton, B.H., Lüscher, B. (2008) Substrate-assisted catalysis by PARP10 limits its activity to mono-ADP-ribosylation. Mol Cell. 32, 57-69.

Langelier, M.F., Servent, K.M., Rogers, E.E., Pascal, J.M. (2008) A Third Zinc-binding Domain of Human Poly(ADP-ribose) Polymerase-1 Coordinates DNA-dependent Enzyme Activation. The Journal of Biological Chemistry. 283, 4105-4114.

Lesner, A., Shilpi. R., Ivanova, A., Gawinowicz, M.A., Lesniak, J., Nikolov, D., Simm, M. (2009) Identification of X-DING-CD4, a new member of human DING protein family that is secreted by HIV-1 resistant CD4+ T cells and has antiviral activity.

Limauro, D., Fiorentino, G., Bartolucci, S. (2004) How Sulfolobus responds to enviromental stress. In Biochemistry and Molecular Biology in the Thermophilic Archaeon *Sulfolobus Solfataricus* (Farina, B & Faraone Mennella, MR, eds), pp. 105–130. Research Signpost, Kerala, India

Luecke, H., Quiocho, F.A. (1990) High specificity of a phosphate transport protein determined by hydrogen bonds. Nature. 347, 402-6.

Meder, V. S., Boeglin, M., de Murcia, G., Schreiber, V. (2004) PARP-1 and PARP-2 interact with nucleophosmin/B23 and accumulate in transcriptionally active nucleoli. Journal of Cell Science 118, 211-222.

Menissier-de Murcia, J., Molinete, M., Gradwohl, G., Simonin, F., de Murcia, G. (1989) Zinc-binding domain of poly(ADP-ribose)polymerase participates in the recognition of single strand breaks on DNA. J. Mol. Biol. 210, 229–233.

Meyer-Ficca, M.L., Meyer, R.G., Coyle, D.L., Jacobson, E.L., and Jacobson, M.K. (2004) Human poly(ADP-ribose) glycohydrolase is expressed in alternative splice variants yielding isoforms that localize to different cell compartments. *Exp. Cell Res.* 297: 521–532.

Morales, R., Berna, A., Carpentier, P., Contreras-Martel, C., Renault, F., Nicodeme, M., Chesne-Seck, M.L., Bernier, F., Dupuy, J., Schaeffer, C., Diemer, H., Van-Dorsselaer, A., Fontecilla-Camps, J.C., Masson, P., Rochu, D., Chabriere, E. (2006) Serendipitous discovery and X-ray structure of a human phosphate binding apolipoprotein. Structure 14, 601–609.

Nguewaa, P. A., Fuertesb, M.A., Valladaresa, B., Alonsob C., Pérez, J.M. (2005) Poly(ADP-Ribose) Polymerases: Homology, Structural Domains and Functions. Novel Therapeutical Applications. Progress in Biophysics and Molecular Biology,; 88, 143-172.

Oka, S., Kato, J., Moss, J. (2006) Identification and characterization of a mammalian 39-kDa poly(ADP-ribose) glycohydrolase, J. Biol. Chem. 281, 705–713.

Otto, H., Reche, P.A., Bazan, F., Dittmar, K., Haag, F., Koch-Nolte, F. (2005) In silico characterization of the family of PARP-like poly(ADP-ribosyl)transferases (pARTs). BMC genomics, 6 . p. 139. ISSN 1471-2164.

Pantazaki, A. A., Tsolkas, G. P., Kyriakidis, D. A. (2008) A DING phosphatase in *Thermus thermophilus*. Amino Acids. 34, 437–448.

Perera, T., Berna, A., Scott, K., Lemaitre-Guillier, C., Bernier, F. (2008) Proteins related to St. John's Wort p27SJ, a suppressor of HIV-1 expression, are ubiquitous in plants. Phytochemistry 69: 865–872.

Plekhanov, AY. (1999) Rapid staining of lipids on thin-layer hromatograms with amido black 10B and other water-soluble stains. Anal Biochem. 271,186-7.

Rabilloud, T. (1992) A comparison between low background silver diammine and silver nitrate protein stains. Electrophoresis 13,429–439.

Reddy, T. R., and Suryanaryana, T. (1989) Archaebacterial histone-like proteins: Purification and characterization of helix stabilizing DNA binding proteins from the acidothermophile *Sulfolobus acidocaldarius*. J Biol Chem. 264, 17298-308.

Rochu, D., Chabriere, E., Elias, M., Renault, F., Clery-Barraud C., Masson, P. (2008) Stabilisation of Active Form of Natural Human PON1 Requires HPBP. Proteins And Cell Regulation. 6, 171-183.

Rochu, D., Masson, P., Fontecilla-Camps, J.C., Chabrière, E. (2006) Crystallization and preliminary X-ray diffraction analysis of human phosphate-binding protein. Acta Crystallograph Sect F Struct Biol Cryst Commun 62: 67–69

Rochu, D., Renault, F., Elias, M., Hanne, S., Cléry-Barraud, C (2007) Functional states, storage and thermal stability of human paraoxonase: Drawbacks, advantages and potential. Toxicology 142.

Roppelt, V., Hobel, C.F., Albers, S.V., Lassek, C., Schwarz, H., Klug, G., Evguenieva-Hackenberg, E. (2010) The archaeal exosome localizes to the membrane. FEBS Lett. 584, 2791-5.

Schreiber, V., Molinete, M., Boeuf, H., de Murcia, G., Menissier-de Murcia, J. (1992) The human poly(ADP-ribose)polymerase nuclear localization signal is a bipartite element functionally separate from DNA binding and catalytic activity. EMBO J. 11, 3263–3269.

Scott, K., Wu, L. (2005) Functional properties of a recombinant bacterial DING protein: comparison with a homologous human protein. Biochim Biophys Acta 1744, 234–244.

Sharp, M. D., Pogliano, K. (1999). From the Cover: An in vivo membrane fusion assay implicates SpoIIIE in the final stages of engulfment during *Bacillus subtilis* sporulation. *Proc. Natl. Acad. Sci. USA* 96: 14553-14558

She, Q., Singh, R.K., Confalonieri, F, Zivanovic Y, Allard G, Awayez MJ, Chan-Weiher CC, Clausen IG, Curtis BA, De Moors A, Erauso G, Fletcher C, Gordon PM, Heikamp-de Jong I, Jeffries AC, Kozera CJ, Medina N, Peng X, Thi-Ngoc HP, Redder P, Schenk ME, Theriault C, Tolstrup N, Charlebois RL, Doolittle WF, Duguet M, Gaasterland T, Garrett RA, Ragan MA, Sensen CW, Van der Oost J. (2001) The complete genome of the crenarchaeon Sulfolobus solfataricus P2. Proc Natl Acad Sci U S A. 98, 7835-40.

Shieh, W.M., Amé, J.C., Wilson, M.V., Wang, Z.Q., Koh, D.W., Jacobson, M.K., Jacobson, E.L. (1998) Poly(ADP-ribose) polymerase null mouse cells synthesize ADP-ribose polymers. J. Biol. Chem. 273, 30069–30072.

Shih, D.M., Gu, L., Xia, Y.R., Navab, M., Li, W.F. (1998) Mice lacking serum paraoxonase are susceptible to organophosphate toxicity and atherosclerosis. Nature 394, 284–287.

Sutravea, P., Shafera, B. K., Stratherna J.N., Hughes, S.H. (1994) Isolation, identification and characterization of the FUN12 gene of Saccharomyces cerevisiae.

Teira, E., Reinthaler, T., Pernthaler, A. Pernthaler, J., Herndl, G.J. (2004) Combining catalyzed reporter deposition-fluorescence in situ hybridization and microautoradiography to detect substrate utilization by bacteria and archaea in the deep ocean. Appl. Environ. Microbiol.; 70, 4411-4414.

Woese, C. R., Kandlert, O., Wheelis, M.L. (1990) Towards a natural system of organisms: Proposal for the domains Archaea, Bacteria, and Eucarya. Proc. Nati. Acad. Sci. USA. 87, 4576-4579.

Woodhouse, B.C., Dianov, G.L. (2008) Poly ADP-ribose polymerase-1: An international molecule of mystery. DNA Repair 7, 1077–1086.

Yamanaka, H., Penning, C.A., Willis, E.H., Wasson, D.B., Carson, D.A. (1988) Characterization of human poly(ADP-ribose) polymerase with autoantibodies, J. Biol. Chem. 263 3879–3883.

Zhang, X.X., Scott, K., Meffin, R., Rainey, P. (2007). Genetic characterization of psp encoding the DING protein in *Pseudomonas fluorescens* SBW25. BMC Microbiol 7, 114

PUBBLICAZIONI

De Maio A., **Porzio E.**, Romano I., Nicolaus B., Faraone Mennella M.R. Purification of the poly-ADP-ribose polymerase-like thermozyme from the archaeon *Sulfolobus solfataricus*.
"Methods In Molecular Biology on poly-ADP-ribose"; ISSN: 1064-3745, p.1-25 (2010) *in press.*
(CHAPTER 28)

TABLE OF CONTENT

INTRODUCTION.

Part I: Biochemical approaches *in vitro* and *in vivo*

CHAPTER 1. Girish M Shah, Febitha Kandan-Kulangara, Alicia Montoni, Rashmi G. Shah, Julie Brind'Amour and Momchil D. Vodenicharov
Approaches to detect PARP-1 activation in cells and tissues

CHAPTER 2. Rafael Alvarez-Gonzalez and Myron K. Jacobson
Quantification of poly(ADP-ribose) *in vitro*: Determination of the (ADP-ribose) chain length and branching pattern

CHAPTER 3. Opeyemi A. Olabisi and Chi-Wing Chow
Assay for Protein Modification by Poly-ADP-Ribose *in vitro*

CHAPTER 4. Michael Hottiger
TBA

CHAPTER 5. Maria Malanga and Felix R. Althaus
Non-covalent protein interaction with poly(ADP-ribose)

CHAPTER 6. Yingbiao Ji
Non-covalent pADPr interaction with protein and competition with RNA for binding to protein

CHAPTER 7. Jean-Philippe Gagné, Jean-François Haince, Émilie Pic and Guy G. Poirier
Affinity-based assays for the identification and quantitative evaluation of noncovalent poly(ADP-ribose)-binding proteins

CHAPTER 8. Yi-Chen Lai, Rajesh K. Aneja, Margaret A. Satchell, and Robert S.B. Clark